Marine and Petroleum Geology 129 (2021) 105074

Contents lists available at ScienceDirect

Marine and Petroleum Geology

journal homepage: www.elsevier.com/locate/marpetgeo

Research paper

Sequence stratigraphy and organic geochemistry: An integrated approach to understand the anoxic events and paleoenvironmental evolution of the Ceará basin, Brazilian Equatorial margin

Ana Clara B. de Souza [a,*], Daniel R. do Nascimento Jr. [b], Francisco Nepomuceno Filho [c], Alessandro Batezelli [d], Felipe H. dos Santos [e], Karen M. Leopoldino Oliveira [f], Narelle Maia de Almeida [b]

[a] Postgraduate Program in Geology, Federal University of Ceará (UFC), Fortaleza, Ceará, Brazil
[b] Department of Geology, Federal University of Ceará (UFC), Fortaleza, Ceará, Brazil
[c] Department of Physics, Federal University of Ceará (UFC), Fortaleza, Ceará, Brazil
[d] Institute of Geosciences, State University of Campinas (UNICAMP), Campinas, São Paulo, Brazil
[e] Institute of Geosciences and Engineering, Federal University of Western Pará (UFOPA), Santarém, Pará, Brazil
[f] Post-doctoral Researcher of the Federal University of Rio Grande Do Norte (UFRN), Natal, Rio Grande do Norte, Brazil

ARTICLE INFO

Keywords:
Stratigraphic sequence
Transgressive-regressive sequences
Relative hydrocarbon potential
Geochemical markers
Cretaceous anoxic events

ABSTRACT

An organic geochemical investigation combined with sequence stratigraphy was performed in the Ceará Basin, an offshore basin located in Northeastern Brazil. The information available from 30 well logs (gamma-ray, resistivity, density), besides geochemical (TOC, and pyrolysis indexes) and isotopic ($\delta^{13}C$) data, aided the preparation of a dataset for this study. The application of sequence-stratigraphic methods helped classify and correlate seismic and organic facies. Four key petroleum source-rock units were identified, from the oldest to the youngest: (1) Mundaú Formation – top of the Rift Sequence (Berriasian-Aptian); (2) Paracuru Formation – Breakup Sequence (Aptian-Albian); (3) Itapajé Member of the Ubarana Formation – Continental Drift Sequence (Albian-Turonian), and (4) Uruburetama Member of the Ubarana Formation – Continental Drift Sequence (Turonian-Maastrichtian). The geochemical characteristics of the Mundaú Formation (high total organic carbon (TOC), hydrogen index (HI), relative hydrocarbon potential (RHP = (S1 + S2)/TOC)) point to a typical transgressive sequence. Six transgressive-regressive (T-R) cycles were recognized in the entire Paracuru Formation. The best geochemical marker is related to the top of the Paracuru Formation. This stratigraphic unit can be correlated to a major anoxic event and is the best source rock of this basin. Evaporitic facies found in this top section, maximum RHP values (anoxic conditions), and maximum flooding surfaces related to transgressive events characterize this interval. Moreover, the wide spatial cover of organic-rich rocks, carbon isotopic data, and the recognition of favorable characteristics for anoxia in other basins of the Equatorial Margin are suggestive of the Aptian-Albian Oceanic Anoxic Event (OAE-1b) occurring in the Ceará Basin. The Ubarana Formation represented by the Uruburetama Member and the Itapajé Member yields the least promising source rocks. However, high TOC values suggest the occurrence of the late Cenomanian–early Turonian Oceanic Anoxic Event (OAE-2), when organic-rich strata started to deposit in deep-water regions. The predominance of a regressive interval in the Uruburetama Member points to oxic or sub-oxic conditions. Additionally, the correlations between the Brazilian Equatorial Margin and its African counterpart, and the organic geochemical characterization allied to the definition of depositional systems for these regions proved to be useful for oil exploration.

1. Introduction

Oceanic anoxic events (OAEs) have been characterized in sedimentary records by levels of widespread organic enrichment induced by stimulated primary productivity and nutrient accumulation, derived from both terrestrial or planktonic sources. The broad spatial

* Corresponding author. Geology Graduate Program, Federal University of Ceará (UFC), Pici University Campus, Building 912, Fortaleza, Ceará, 60440-554, Brazil.
E-mail addresses: souzaanaclarageologia@gmail.com, anaclarageologia@alu.ufc.br (A.C.B. Souza).

https://doi.org/10.1016/j.marpetgeo.2021.105074
Received 20 January 2021; Received in revised form 29 March 2021; Accepted 6 April 2021
Available online 20 April 2021

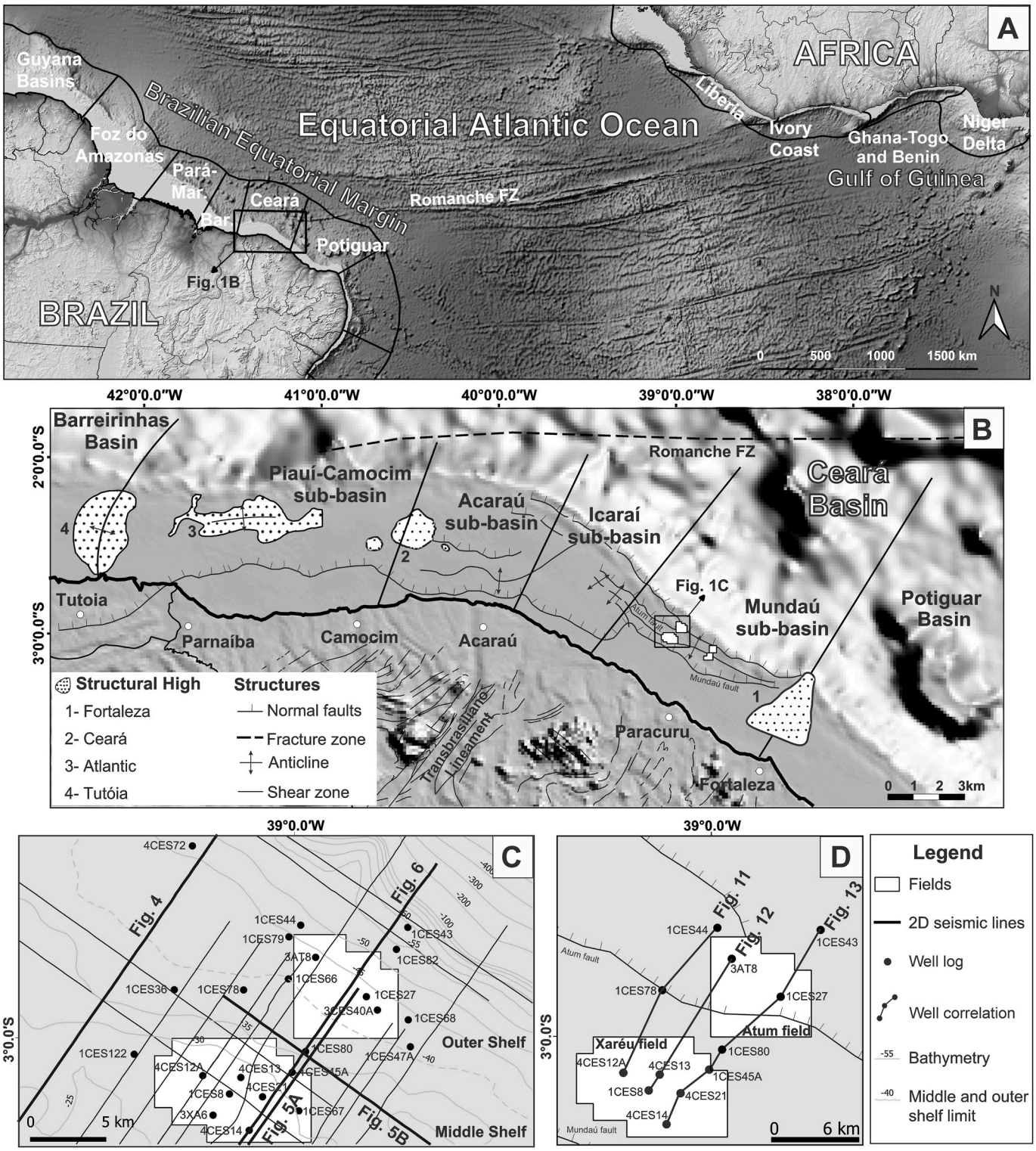

Fig. 1. Location of the study area. A) Equatorial Atlantic seafloor map highlighting the Romanche Fracture Zone, the Brazilian Equatorial Margin on the South American continent northeastern coast, composed of the Potiguar, Ceará (study area), Barreirinhas (Bar), Pará-Maranhão (Pará-Mar) and Foz do Amazonas sub-basins (modified after Morais Neto et al., 2003) and the conjugate West African margin on the African continent western coast, represented by the Gulf of Guinea Province, which includes the Niger River Delta, Ghana-Togo, Benin, Ivory Coast, and Liberia basins (modified after Brownfield and Charpentier, 2006). B) Detail of the Brazilian Equatorial Margin highlighting the Ceará Basin limits, sub-basins, structural elements, and production fields. C) Bathymetric map showing the location of four regional 2D seismic profiles (indicated as Fig. 4–6) and wells used in this study (see Table 1). D) Location of the 11 wells selected for lateral correlations and three seismic profiles (indicated as Figs. 11–13).

occurrence and geochemical $\delta^{13}C$ anomalies indicate that marine waters were relatively depleted in oxygen, causing changes in fossiliferous assemblages (*c.f.* Schlanger and Jenkyns, 1976; Jenkyns et al., 1999; Bralower et al., 1994; Gröcke et al., 1999; Jenkyns, 2010; Soua, 2016; Rodrigues et al., 2019). The Cretaceous OAEs are generally associated with eustatic transgressions, which are understood as intense flooding events (Schlanger and Jenkyns, 1976, 2007; Haq et al., 1987; Soua and Tribovillard 2007; Tiraboschi et al., 2009; Jenkyns, 2010; Bastos et al., 2020). These transgression events are mostly related to specific eustatic sea-level rises and they can influence source-rock distribution and hydrocarbon generation (e.g., Jenkyns, 1980; Haq et al., 1987; Wagner et al., 2007; Jenkyns, 2010; Slatt and Rodriguez 2012; Haq et al., 2014; Rodrigues et al., 2019).

Source-rock organic geochemical characterization includes determining and quantifying, respectively, type and amount of organic matter and, after that, its hydrocarbon generation potential (Espitalié et al., 1977; Peters, 1986; Katz, 1983, 2005; Tissot and Walte, 1984; Anders, 1991; Hunt et al., 2002; Dembicki, 2009; Jarvie, 2012; Hart and Steen, 2015). The relative hydrocarbon potential is a geochemical parameter that reflects the oxygenation conditions of the depositional environment (Fang et al., 1993; Slatt and Rodriguez, 2012; Miceli-Romero and Philp, 2012). It can be related to relative sea-level fluctuations within a sequence-stratigraphic context. From a geochemical approach, Pasley and Hazel (1990), Pasley (1991), Pasley et al. (1991), Fang et al. (1993), Creaney and Passey (1993), Hart et al. (1994), Harbor (2011), and Gürgey and Bati (2018) noted that changes in kerogen type is a useful parameter in outlining transgressive and regressive sequences. In a broad sense, recent studies carried out in marine and lacustrine environments have shown that Rock-Eval parameters, geochemical proxies (i.e., total organic carbon (TOC), hydrogen index (HI), relative hydrocarbon potential (RHP = (S1 + S2)/TOC)), and stable isotopes can also be used to understand sea-level changes in related depositional setting (Bohacs et al., 2000; Harris et al., 2004; Slatt and Rodriguez, 2012; Gambacorta et al., 2020).

Sequence stratigraphy of fine-grained sedimentary rocks combined with organic facies characterization is a powerful tool for regional to local stratigraphic correlations from well logs, seismic reflection records and geochemical analysis (Creaney and Passey, 1993; Fang, 2011). Sequence stratigraphy may give clues about the time interval for the generation of organic-rich and organic-poor strata related to transgressive-regressive sequences (Hancock and Kauffman, 1979; Van Wagoner et al., 1987; Pasley and Hazel, 1990; Pasley et al., 1991; Emery and Myers, 2009; Slatt, 2013; Kaixuan et al., 2017; Embry and Johannessen, 2017). The variation of TOC contents provides a critical clue for locating key boundaries within shale-dominated successions (Loutit et al., 1988; Creaney and Passey, 1993; Tayson, 2001; Freire and Monteiro, 2013). In addition, maximum flooding surfaces can be characterized by low sedimentation rates, and constant supply of organic-rich material under anoxic conditions that favor minimum decomposition of organic matter (Wignall, 1991; Creaney and Passey, 1993; Catuneanu et al., 2011). Additionally, an integrated approach using geochemistry and sequence stratigraphy is a reasonable way for assessing subsurface basin fills, focusing on environmental conditions (Adatte et al., 2002; Lüning et al., 2004; Slatt and Rodriguez, 2012; Daher et al., 2015; Peng et al., 2016; Omodeo-Salé et al., 2016; Delgado et al., 2018; Shekarifard et al., 2019; Adeoye et al., 2020).

Despite recent advances in the definition of the stratigraphic framework of the Ceará Basin via geochemical approaches (e.g., Maia de Almeida 2020a; 2020b; Leopoldino Oliveira et al., 2020; Souza et al., 2021), issues related to the paleoenvironmental significance of organic-rich rocks still require further study. Thus, the objective of this paper is to present an integrated study of sequence stratigraphy and organic geochemical characterization of transgressive and regressive cycles that occurred during the Cretaceous of the Ceará Basin. This approach enabled to estimate sea-level variations that led to environmental changes, and to construct models for organic facies deposition linked to the tectonic evolution of the Equatorial Atlantic Ocean. The discussions focus on the assessment of paleoenvironmental dynamics and the regional occurrence, significance, and characteristics of oceanic anoxic events in the Brazilian Equatorial Margin and its African counterpart.

2. Geological background

2.1. The Ceará Basin

The Ceará Basin is an offshore basin located in Northeastern Brazil and belongs to a series of offshore basins of the Brazilian Equatorial Margin (Costa et al., 1990; Condé et al., 2007). The Tutóia and Fortaleza Highs separate the Ceará Basin from the Barreirinhas and Potiguar basins (Fig. 1B). The Precambrian Borborema Province marks the south limit in the continent. In the north limit, two tectonic and geomorphologic features stand out: i) the Ceará Guyot, a volcanic feature that is considered as an extension of the Fernando de Noronha Chain (Costa et al., 1990; Beltrami et al., 1994; Morais Neto et al., 2003; Condé et al., 2007), and ii) the Romanche Fracture Zone, which extends to its conjugate African margin. There, the West African basins of the Gulf of Guinea Province extend from the western border of the Niger River delta to the eastern part of Ghana (Brownfield and Charpentier, 2006) (Fig. 1A).

The Ceará Basin is subdivided into four sub-basins, from west to east: Piauí-Camocim, Acaraú, Icaraí and Mundaú (Fig. 1B). This subdivision is based on different aspects of the stratigraphic evolution and different tectonic-sedimentary regimes (Zalán et al., 1985; Costa et al., 1990; Morais Neto et al., 2003; Condé et al., 2007), and also on structural features, such as the Ceará High, the Transbrasiliano Lineament extension and the Mundaú sub-basin border fault inflection from west to east (Fig. 1B) (Mohriak, 2003; Morais Neto et al., 2003; Condé et al., 2007). The Mundaú sub-basin stratigraphic record, which ranges from Early Cretaceous to recent, is the thickest of the Ceará Basin. It encompasses the Xaréu, Atum, Curimã, and Espada fields (Beltrami et al., 1994; Morais Neto et al., 2003; Pessoa Neto et al., 2004; Condé et al., 2007). All these fields are exploited for oil and gas.

2.2. Evolution of the brazilian Equatorial Margin

The geodynamic evolution of the Ceará Basin is related to the breakup of Western Gondwana, which resulted in the separation of the South American and African plates in the Early Cretaceous (Mascle et al., 1988; Almeida et al., 2000; Matos, 2000; Mohriak et al., 2003; Davison et al., 2015). The process started with thinning of the continental lithosphere and mantle exhumation. Plate tectonics at this stage is characterized by rifting, block faulting, subsidence and pulling apart of the crystalline basement, which created a series of horsts and grabens and deposition settings controlled by the Romanche Fracture Zone (Mascle et al., 1997; Matos, 2000; Tamara et al., 2020). This stage started in the Barremian (?)–early Aptian with deformation distributed within E−to ENE-trending intracratonic basins filled with non-marine sediments (Mascle et al., 1988; Azevedo, 1991; Matos, 2000).

Plate kinematic models suggest that accretion of oceanic crust in isolated basins started in the early Albian (120-105 Ma) (Heine et al., 2013; Moulin et al., 2010) and was coeval with transtension along the Ceará transform margins (Matos 2000; Davison et al., 2015; Tamara el al., 2020). This evolutionary model relates to the Equatorial Atlantic Ocean opening, which continued creating more space for the accommodation of sediments. This led to the initial breakup of the continents, causing the first marine transgression. It was succeeded by regressions that caused sedimentation and formation of claystones, mudstones, shales, and sandstones in depositional environments ranging from fluvio-deltaic to marine develops (Matos, 2000; Heine and Brune, 2014; Davison et al., 2015). This interval was reported in the Gulf of Guinea Province, which accredited their similar geologic histories suggesting

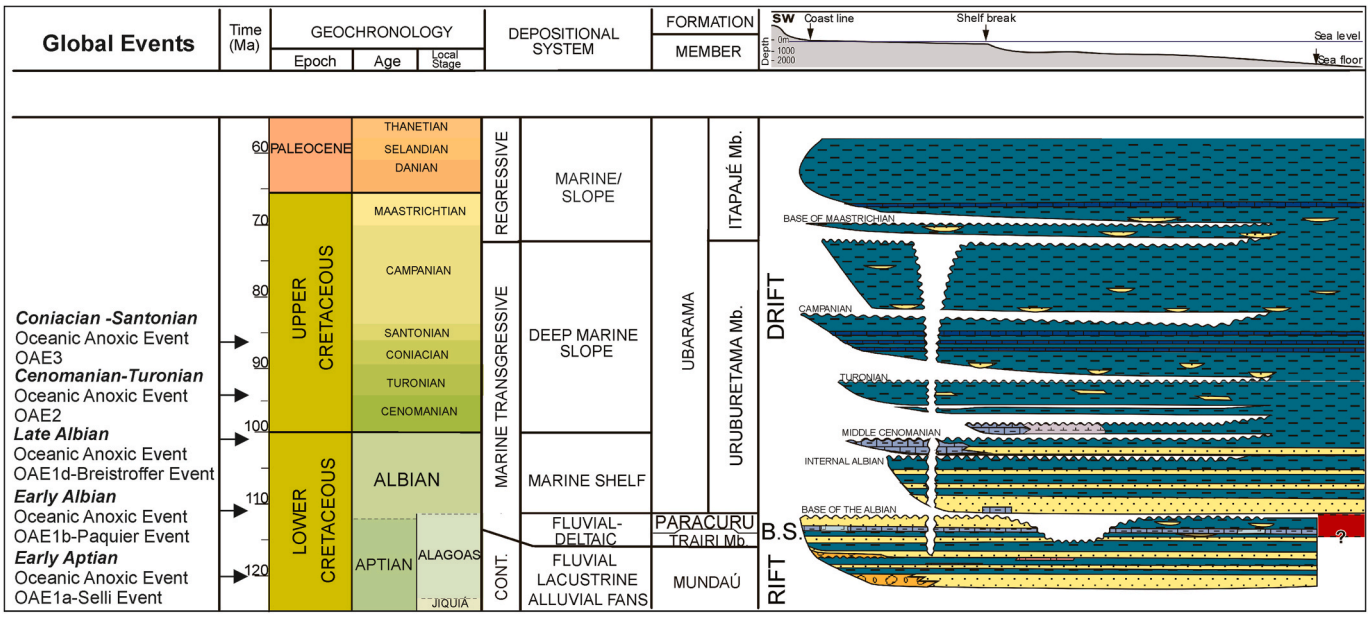

Fig. 2. Nomenclature of the main Cretaceous Oceanic Anoxic Events (OAEs) according to Jenkyns (2010). The OAEs are correlated with the chronostratigraphic chart, depositional environments, and formations of the Ceará Basin (compiled from Condé et al., 2007).

that the two continents were in close proximity (Brownfield and Charpentier, 2006; Mohriak et al., 2003).

Deep marine environments developed with ocean spreading initiating at approximately 110 Ma (Matos, 2000; Heine and Brune, 2014). A change in plate-movement vectors must have occurred near the end of the Albian. Inversion of transtensional basins and the formation of transpressional belts along the Ceará Basin has been attributed to late Albian–Cenomanian contraction driven by changes in the extension direction, and relative movement between South America and West Africa (Mascle and Blarez, 1987; Azevedo, 1991). Final separation of the continental lithosphere corresponding to South America and Africa occurred at 104 Ma along the western Ivory Coast margin and at 94 Ma along the Ghana–Ivory Coast margin, together with migration of the oceanic spreading centers along the respective transform margins at 96 and 74 Ma, respectively (Szatmari et al., 1987; Mascle and Blarez, 1987; Azevedo, 1991; Heine et al., 2013; Nemčok et al., 2013).

For the African counterpart, analogous to the Brazilian Equatorial Margin, three tectonic evolution stages are reported: (1) a Lower Cretaceous pre-transform stage, represented by continental to marginal marine rocks; (2) a lower Cretaceous to late Albian syn-transform stage, and (3) a Cenomanian to Holocene transform stage (Brownfield and Charpentier, 2006).

2.3. The Ceará Basin stratigraphic sequence

Three Barremian (?)–recent sequences compose the Ceará Basin; the rift (continental), post-rift (transitional) or breakup, and the drift (open-marine) sequences (Szatmari, 1987; Beltrami et al., 1994; Condé et al., 2007; Maia de Almeida, 2020a) (Fig. 2). The Mundaú Formation (Berriasian? to Aptian) encompasses the syn-rift sequences of the Mundaú Sub-Basin and is composed of fluvial-deltaic and lacustrine deposits (Beltrami et al., 1994; Condé et al., 2007; Holz et al., 2017). Sandstones and shales of the Mundaú Formation represent the continental sedimentation of the Ceará Basin. The Paracuru Formation (~115 Ma) overlies these deposits and represents fluvial-deltaic to lacustrine siliciclastic sedimentation. The Trairí Member of the Paracuru Formation stands out for being composed of carbonates and evaporites (Beltrami et al., 1994; Conde et al., 2007).

The Paracuru Formation defines the first marine ingression in the Ceará Basin (Regali et al., 1989; Costa et al., 1990; Beltrami et al., 1994; Condé et al., 2007) and more recently it has characterized as a breakup sequence *sensu* Soares et al. (2012) (Leopoldino Oliveira et al., 2020; Maia de Almeida et al., 2020a). The following Ubarana, Tibal and Guamaré formations represent the drift sequence sedimentation in open marine settings. The Ubarana Formation is subdivided into two distinct members in the study area. The Uruburetama Member (~110 Ma to 75 Ma), composed of thin shale beds, was deposited on an unconformity on top of the Paracuru Formation and records a transgression event. The Itapajé Member (~75 Ma to 65 Ma) overlies the Uruburetama Member, and is composed of thick turbidite layers, which correspond to a regressive marine phase, attested by basinward prograding movements (Costa et al., 1990; Beltrami et al., 1994; Condé et al., 2007; Rios and Picanço, 2018; Maestrelli et al., 2020).

A major NW-SE trending fault, known as the Mundaú Fault, structurally limits the Mundaú Sub-basin (Fig. 1D) (Azevedo, 1991; Pessoa Neto et al., 2004; Leopoldino Oliveira et al., 2020; Maia de Almeida et al., 2020b). The boundary faults that limit the Xaréu and the Atum oil fields compose a series of normal faults with listric geometry. Tilted blocks trending NW-SE and dipping NE were formed during the rifting phase (Costa et al., 1990; Pessoa Neto et al., 2004; Leopoldino Oliveira et al., 2020; Maia de Almeida et al., 2020b). The top of grabens and horsts thus formed was later eroded. Previous interpretations correlated this angular unconformity known as Electric Mark 100 with a period of regional flooding that affected the Ceará Basin during the lower Aptian, during which time the geodynamic evolution of the Mundaú Sub-basin was predominantly subjected to a distensional regime in the shallower platform and slope.

Some researchers have approached the Ceará Basin evolution via sequence stratigraphy. Hashimoto et al. (1987), applying event stratigraphy, made the stratigraphic and paleoenvironmental characterization of the Alagoas Stage, which, according to the authors, ranges from the top of the Mundaú Formation to the top of the Paracuru Formation. The authors also recognized transgressive and regressive successions that correlate laterally within the Ceará Basin context. Regali (1989), using lateral correlations, characterized the first marine ingression and evaporite deposition in the late Aptian. Costa et al. (1990) and Pessoa Neto et al. (2004), based on seismic interpretation, illustrated the main relationships between stratigraphic sequence and discordances for the Xaréu field. Beltrami et al. (1994), Morais Neto et al. (2003), and Condé et al. (2007) updated the Ceará Basin chronostratigraphic chart

including the major geological events and sedimentary successions.

2.4. Previous geochemical studies

In the 1980's, the Brazilian Petroleum Corporation – Petrobras authored the first reports containing geochemical data for the Ceará Basin. In these reports, the Mundaú Sub-basin is presented as prone for hydrocarbon generation, and the Paracuru Formation is indicated as the best source-rock (e.g., Mello et al., 1984). Later, oil generation and migration aspects were presented by Costa et al. (1990). ANP (2017) summarized kerogen types and TOC contents for the Mundaú and Paracuru Formation. Recent research on the Brazilian Equatorial Margin (Pellegrini and Ribeiro, 2018; Maia de Almeida et al., 2020a; Leopoldino Oliveira et al., 2020; Souza et al., 2021) and its counterpart in Africa, the West Africa Margin (Brownfield and Charpentier, 2006; Adeoye et al., 2020), has presented geochemical data on the source rocks.

New publications on the deep-water domain of the Ceará Basin have presented a conventional geochemical characterization (kerogen analysis, hydrogen index, total organic carbon) of the Mundaú, Paracuru and Ubarana formations (e.g., Souza et al., 2021). Geochemical analyses of autochthonous hydrocarbon show that kerogen is predominantly of type II and III and reveal fair to excellent potential for oil generation (Maia de Almeida et al., 2020a). Regarding maturity windows, Leopoldino Oliveira et al. (2020) classified Aptian to Turonian samples as mature to post mature. The majority of the samples were of organic matter type II and some of type III. The Ubarana Formation (Turonian) was considered to contain autochthonous marine organic matter with terrestrial contribution, deposited in a reducing environment favorable to oil and gas generation (Leopoldino Oliveira et al., 2020).

Additionally, the deposition of organic-rich sediments in the Mundaú Formation was strongly controlled by half-graben systems, specifically close to border faults in proximal areas (Souza et al., 2021). The Paracuru Formation presents the best source rock in the Ceará Basin, which is characterized by abundant organic matter and indicating a high hydrocarbon potential for these rocks considered oil and gas-prone (Souza et al., 2021). The Ubarana Formation, represented by the Uruburetama and the Itapajé members, contains less promising source rocks. These members yielded immature to early oil-window thermal conditions (Souza et al., 2021). Comparing the continental shelf area and the deep-water domain, the source rocks belong both areas indicate large resemblance (Leopoldino Oliveira et al., 2020; Souza et al., 2021).

3. Dataset and methodology

3.1. Available data

The Brazilian Agency for Petroleum, Natural Gas and Biofuels (ANP) provided all dataset presented in this study. Fifteen regional poststack-migrated 2D seismic data were used for regional stratigraphic interpretation (Fig. 2C). The seismic survey in which these data were acquired dates from 1980 to the 1990's. Vertical resolution of the 2D seismic lines is 22 m. Frequency ranged from 40 to 70 Hz, with dominant 40-Hz frequency and 4-ms sampling. The data were interpreted in two-way travel time (TWT) and the stratigraphy was calibrated with well-log data. Sonic (DT), density (ROHB) and check-shot were also used for comparison with synthetic seismograms to confirm or modify well-to-

Table 1
Well logs selected for the preparation of the dataset used in this study. Fig. 1B presents the spatial distribution of the wells.

Well	Location	Oil field	Year	Classification	Main Objective	TOC # of samples	Pyrolysis # of samples	Check Shots
3 AT 8	Outer shelf	Atum	1985	Extension for oil production	Description of sequences (Figs. 9 and 12) and well-to-seismic calibration	112	103	42
1 CES 44	Outer shelf		1980	Sub-commercial oil production	Description of sequences (Figs. 10 and 11)	114	98	
1 CES 80	Middle shelf		1983	Dry	Description of sequences (Figs. 8 and 13)	69	56	
1 CES 8	Middle shelf	Xaréu	1977	Discovery of oil field	Description of sequences (Figs. 7 and 12) and isotope data	237	151	
4 CES 12A	Middle shelf	Xaréu	1977	Sub-commercial oil production	Well-log correlation (Fig. 11)	114	86	
4 CES 21	Middle shelf	Xaréu	1978	Sub-commercial oil production	Well-log correlation (Fig. 13) and isotope data	48	45	
4 CES 14	Middle shelf	Xaréu	1977	Sub-commercial oil production	Well-log correlation (Fig. 13) and isotope data	39	32	
4 CES 13	Middle shelf	Xaréu	1977	Sub-commercial oil production	Well-log correlation (Fig. 12)	86	32	
1 CES 45A	Middle shelf	Xaréu	1980	Sub-commercial oil production	Well-log correlation (Figs. 5, 6 and 13) and well-seismic calibration	64	54	14
1 CES 78	Middle shelf		1982	Sub-commercial oil production	Well-log correlation (Fig. 11)	144	127	
1 CES 27	Outer shelf	Atum	1979	Discovery of oil field	Well-log correlation (Fig. 13) and well-seismic calibration	83	54	14
1 CES 43	Outer shelf		1981	Dry	Well-log correlation (Figs. 6 and 13) and well-seismic calibration	98	91	19
3 CES 47A	Outer shelf		1980	Dry	Well-seismic calibration			6
1 CES 67	Middle shelf	Xaréu	1981	Sub-commercial oil production	Well-seismic calibration			18
4 CES 72	Outer shelf		1982	Dry	Well-seismic calibration (Fig. 4)	70	34	10
1 CES 82	Outer shelf		1982		Well-log interpretation	156	147	
1 CES 68	Outer shelf		1982	Sub-commercial oil production	Well-log interpretation	109	105	
1 CES 79	Outer shelf		1982	Sub-commercial oil production	Well top information and seismic interpretation	23	18	
1 CES 36	Middle shelf		1979	Dry	Well top information and seismic interpretation			
1 CES 122	Middle shelf		1994	Dry	Well top information and seismic interpretation			

seismic calibration (Bassiouni, 1994) (see Table 1 with data available). Interpretation was based on attributes of the seismic data, such as reflection amplitude and continuity and wavelet frequency. Twenty wells with gamma-ray (GR), resistivity (ILD), spontaneous potential (SP), neutron (NPHI), caliper (CAL), and lithological data, were available.

The lithostratigraphic and chronostratigraphic dataset used in this study contains the stratigraphic top for each formation and their relative age, respectively. The chronostratigraphic information refers to well-established strata recognized from their biological zones. Sixteen from the twenty wells have chronostratigraphic information, amounting to 434 chronostratigraphic marks. Thus, to construct a more reliable stratigraphic framework, this dataset was checked and combined with those from the chronostratigraphic chart from Condé et al. (2007).

The ANP made available the geochemical database from which the dataset for this study was built. Sixteen well logs were selected for the dataset (Table 1). A total of 1566 samples with TOC values and 1233 pyrolysis data for different sedimentary facies were used in this study. The majority of the samples varied from black to medium-gray shales, siltstones, mudstones and other fine-grained rocks.

The data from the dataset prepared for this study were uploaded to the Petrel E&P platform, whose license was granted by Schlumberger to the Federal University of Ceará (UFC). Petrel was used for the interpretation of the seismic data and recognition of seismic patterns, such as seismic terminations horizons and faults. These features are determined in the time domain (Figs. 4–6). After that, suites of gamma ray, TOC, and geochemical logs aided the delineation of the formations and sequence stratigraphy patterns (Figs. 7–10). Correlation canvas provided by Petrel were used to evaluate hydrocarbon distribution, lateral continuity, and RHP curves that showed RHP correlations with changes in oxic conditions and the interaction with lithofacies stacking patterns (Figs. 11–13).

3.2. Sequence-stratigraphic analysis

Classical concepts of sequence stratigraphy presented by Vail et al. (1977), Mitchum (1988), Van Wagoner et al. (1988) and Milton and Emery (2009) were used to interpret the stratigraphic framework and in the discussions in this study. The seismic stratigraphic interpretation was performed applying Mitchum et al. (1977) seismic facies description methods. Key seismic characteristics used in the seismic stratigraphic analysis include reflection strength and continuity, amplitude, frequency, and configuration (e.g., sigmoidal, oblique, mounded, etc.), and reflection geometries or stratal termination patterns such as onlap, downlap, toplap, and truncation (Vail et al., 1977; Mitchum et al., 1977; Veenken et al., 2006). Reflection configuration, and geometry were used to individualize sedimentary stratification patterns. The stratigraphic correlation was based on facies distribution, lithostratigraphic, chronostratigraphic markers, gamma ray patterns, TOC values, and geochemical data.

Shales, mudstones, and other fine-grained rocks are commonly identified by high gamma-ray (GR) values (Beers, 1945; Schön et al., 2015). These high GR values have been attributed to uranium contents associated with organic matter (Swanson, 1960; Hesselbo, 1996). For sequence stratigraphy analysis many researchers have pointed to coincidences between the occurrence of organic-rich intervals and deposition during transgression (Vail et al., 1977; Demaison and Moore, 1980; Dean and Arthur, 1989; Pasley 1991; Emery and Myers, 2009; Slatt and Rodrigues, 2012). For the identification of these intervals in the Ceará Basin, T-R sequences were interpreted. These sequences are formed by transgressive systems tracts overlain by regressive systems tracts (Embry and Johannessen, 1993, 2017; Ashton, 2002; Mancini and Pucket, 2005; Catuneanu, 2009, 2019; Lü et al., 2010; Jacquin and Graciansky, 2012; Gürgey and Bati, 2018). The maximum regressive surface (MRS) marks the upper boundary of a regressive systems tract and represents changes toward a transgression depositional regime (Embry et al., 2007; Embry and Johannessen, 2017). In transgressive systems tracts there is a base level rise, and this change reflects a reduced supply of sediments and migration of the shoreline landward. Contrarily to the MRS, the maximum flooding surface (MFS) is the surface that delimits changes from transgressive systems tract to regressive systems tracts (Embry et al., 2007; Embry and Johannessen, 2017). From this boundary, there is an increase in sediment supply resulting in coarse sediment progradation across the shelf, and a base level fall. Thus, lateral extension was described using lateral correlation integrated to the geochemical markers in the interpreted T-R sequences.

3.3. The geochemical dataset

The geochemical dataset prepared for this study encompasses the following parameters: Total Organic Carbon (TOC), Rock-Eval pyrolysis indexes (free hydrocarbons – S1; hydrocarbon generative potential – S2; hydrogen index – HI; oxygen index – OI; temperature at the maximum of the S2 peak – T_{max}), and other parameters calculated using the rock-eval indexes, as detailed below.

The Total Organic Carbon (TOC) represents the organic carbon content in weight percent (wt.% TOC). It is a semi-quantitative information on the organic matter contained in a rock sample, regardless the carbonate fraction (Tissot and Welte, 1984; Hart and Steen, 2015). It represents the biogenically-derived carbon and reflects the production and preservation conditions in a depositional environment (Espitalié et al., 1984; Jarvie, 1991; Hunt, 1995; Hart and Steen, 2015).

The Rock-Eval pyrolysis simulates the natural conditions of organic matter metagenesis and catagenesis for source-rock characterization and evaluation (Espitalié et al., 1977; Hunt et al., 2002). A rock sample is placed in a chamber filled with inert gas. The sample is gradually heated according to a heating program. A flame ionization detector senses organic compounds emitted during each heating stage, while sensitive infrared detectors measure CO and CO_2 (Espitalié et al., 1977). The quantification of the amounts of these gases provides the following indexes: S1, the first peak of the pyrolysis and expressed in milligrams of hydrocarbons per gram of rock, represents the amount of free hydrocarbons within organic matter; S2, the second peak of the pyrolysis and also expressed in milligrams of hydrocarbons per gram of rock, represents the amount of hydrocarbons formed during the thermal decomposition of kerogen; S3, expressed in milligrams CO_2 per gram of rock, is the proportion of pyrolyzed CO_2 relative to the oxygen present in the kerogen, and T_{max}, expressed in degrees Celsius, is the temperature at the maximum of the S2 peak (Barker, 1974; Espitalié et al., 1977, 1984; Jarvie, 1991; Behar et al., 2001; Hart and Steen, 2015).

The parameters calculated using the pyrolysis indexes are:

- HI – hydrocarbon index (HI = S2/TOC*100) expressed in milligrams of hydrocarbons (HC) per gram of TOC. It is related to the hydrogen to carbon ratio (H/C), and is used to characterize the origin and maturity of the kerogen of organic matter;
- OI – oxygen index (OI = S3/TOC*100), expressed in milligrams of hydrocarbons (HC) per gram of TOC). It is a parameter that correlates with the oxygen to carbon ratio (O/C);
- GP – genetic potential (GP = S1+S2) is the sum of the values S1 and S2 expressed in milligrams of hydrocarbons (HC) per gram of rock;
- And RHP – relative hydrocarbon potential (RHP = [S1+S2]/TOC*100), which is, among other environmental characteristics, an indicator of oxic/anoxic conditions, as discussed below.

3.4. Anoxic signature

In addition to the classical stratigraphic analysis, the organic geochemical indexes (i.e., TOC, HI, and RHP) are indicative (proxies) of shale deposition, organic matter preservation, persistence of anoxic and oxic conditions, and relative sea-level changes (Harris et al., 2004; Slatt and Rodriguez, 2012; Miceli-Romero and Philp, 2012; Abouelresh and Slatt, 2012; Gürgey and Bati, 2018) (see Fig. 3). The relative

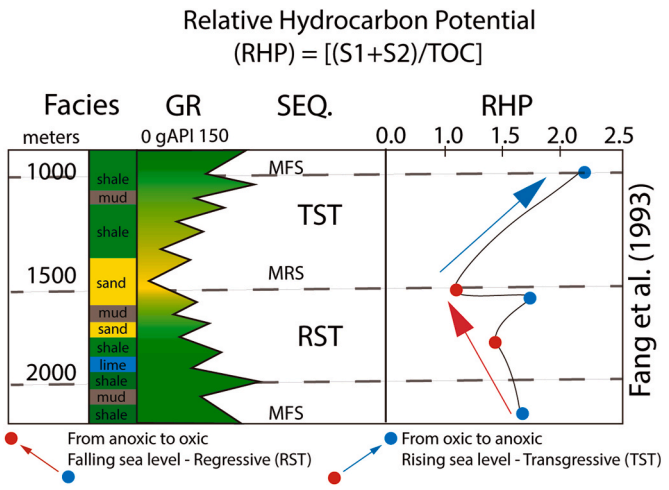

Fig. 3. Schematic profile correlating depth (m), lithofacies, gamma-ray stacking patterns (GR), transgressive (TST) and regressive (RST) sequence tracts, and sequence boundary (maximum flooding surface – MFS and maximum regressive surface – MRS). Relative changes in oxygen levels indicated by the relative hydrocarbon potential (RHP) curves proposed by Fang et al. (1993) (modified after Slatt and Rodriguez, 2012).

hydrocarbon potential (RHP) is a reliable geochemical parameter when it comes to the oxygenation characteristics of depositional systems. It can be associated with sea-level changes within a sequence-stratigraphic setting (Fang, 1993; Slatt and Rodriguez, 2012; Gürgey and Bati, 2018).

This parameter was first used by Fang et al. (1993), who established two main sequences based on RHP. The first represents a vertical, rising-upward change in organic facies, from hydrogen-poor to hydrogen-rich. It indicates a change from oxic to anoxic conditions and sea-level rise, during which time most of the organic matter is preserved (Fig. 3). The second, also vertical but contrarily to the first – a falling-upward change, represents a change from hydrogen-rich to hydrogen-poor organic facies, indicating a change from anoxic to oxic conditions and sea-level fall, and consequently less organic matter is preserved (Fig. 3). Thus, the concept of regressive-transgressive cycles can be applied to sequence stratigraphy.

Furthermore, Creaney and Passey (1993), Hart et al. (1994), Buckner et al. (2009), Slatt et al. (2011), Slatt and Rodriguez (2012), Miceli-Romero and Philp (2012), and Gürgey and Bati (2018) also attest RHP or vertical changes in organic facies as a potential proxy for oxygen conditions and sea-level fluctuations. The RHP curve assessment indicates that there is a positive correlation with the TOC patterns or gamma-ray readings, which are established by a traditional sequence-stratigraphic framework (Miceli-Romero and Philp, 2012). Slatt and Rodriguez (2012) show that maximum RHP values (anoxic conditions) correspond to flooding surfaces, while minimum RHP values (oxic conditions) correlate with the location of sequence and parasequence boundaries. Thus, RHP values are indicative of redox conditions, extent of anoxia in sequence stratigraphy, and the boundary of transgression and regression moments (Abouelresh and Slatt, 2012; Slatt and Rodriguez, 2012; Gürgey and Bati, 2018).

The RHP as an indicator/proxy of anoxic and oxic depositional environments and organic matter preservation is related to anoxic conditions associated with transgressive events (Fang et al., 1993; Gürgey and Bati, 2018). Additionally, in sequence stratigraphy transgressive phases may represent relative sea-level rising. Thus, the results shown by the RHP can also be considered as a fingerprint of relative sea-level fluctuations when traditional information, such as biostratigraphic, seismic, and isotopic data, are lacking or limited (Curiale et al., 1992; Hart et al., 1994; Miceli-Romero and Philp, 2012; Abouelresh and Slatt, 2012; Slatt and Rodriguez, 2012; Gürgey, 2018).

4. Results

4.1. Regional seismic setting

Martins and Coutinho (1981) subdivide the Ceará Basin into three sectors, according to their sedimentological and morphological characteristics: inner shelf (up to 20-m deep), middle shelf (between 20 and 40 m of depth), and outer shelf (from 40 m to the slope segment). The depth of the slope or shelf-breaking zone is 60–70 m (Fig. 1C and D).

The interpretation of dip seismic reflection profile R0003 GRAND NORTH 0222 0506. MIG FIN.395 corroborates the subdivision of the Ceará Basin into inner-, middle- and outer-self domains, which is the zonation adopted in this study (Fig. 4). The most proximal domain corresponds to the inner shelf and to shallow waters (acoustic basement at ~ 500 ms). In this zone, no faulting or sedimentation related to the Mundaú or Paracuru formations occur. The middle-shelf domain is formed by border and listric faults related to the Xaréu field and proximal sedimentation (Fig. 4). The faults in this domain were reactivated throughout the rift to post-rift events without significant changes in attitude. The outer shelf is the last shelf-margin domain. It is correlated with environmental conditions prior to continental breakup. The Atum field is located in this domain, close to the continental slope. As shown in Fig. 4, the Mundaú and Paracuru formations do not seem to be affected by the reactivation of faults.

The structural signature related to the main rifting phase is predominantly composed of NW-SE-trending en echelon and listric faults. The Xaréu and Atum fields are limited by such faults. Other structures, such as negative flowers, anticlinal folds, high-angle normal faults (generating grabens and horsts), mainly affect the Mundaú Formation. Reactivation is recorded in the Paracuru Formation, as sedimentation takes place along major normal faults, revealing active tectonic subsidence during deposition. In the beginning of the drift phase, faulting is ceased, and the Uruburetama Formation represents the last sequence affected by reactivation.

4.2. Key surfaces and sequence-stratigraphic units

The formations and members of the Ceará Basin are subdivided in eleven major seismic stratigraphic subunits or seismic facies. The identification of boundaries and surfaces indicates possible distinct T-R cycles (Fig. 5).

Regional unconformities/horizons are identified, and the sedimentary units are named from bottom to top as shown in the table of Fig. 5C. Seismic units and their boundaries (Horizons) are defined by the occurrence of seismic features such as truncations, onlaps, hiatuses, and distinct surfaces associated with facies changes. The main unconformity/horizon marks the contact between sediment accumulation on the basement and the rift sedimentation. Four subunits are identified in the Mundaú Formation and named 2 A, 2 B, 2C, and 2D from bottom to top. Three subunits are identified in the Paracuru Formation, namely 3 A, 3 B (which corresponds to the Trairí Member) and 2C. The Uruburetama Member of the Ubarana Formation is into subunit 4, and the Itapajé Member into subunits 5. The Tibal and Guamaré Formations are gathered in Subunit 6.

4.2.1. Subunit 1 – the basement

Subunit 1 is located around ~3500–4000 ms TWT. It is overlain by a thick, 2000–2500 ms TWT sedimentary layer named Subunit 2. Subunit 1 is described as a seismic interval characterized by weak, discontinuous, and chaotic reflections, limited by Horizon 1. This highly disrupted reflectors show strong amplitude and variable frequency, characterizing the acoustic basement. The faults extend overlying the basement limit. Onlap-fill facies are recognized onlapping against the fault planes of the border faults. These seismic facies above the basement are characterized by being relatively more parallel and correspond to the sedimentary fill of the Ceará Basin. In the outer shelf, seaward-

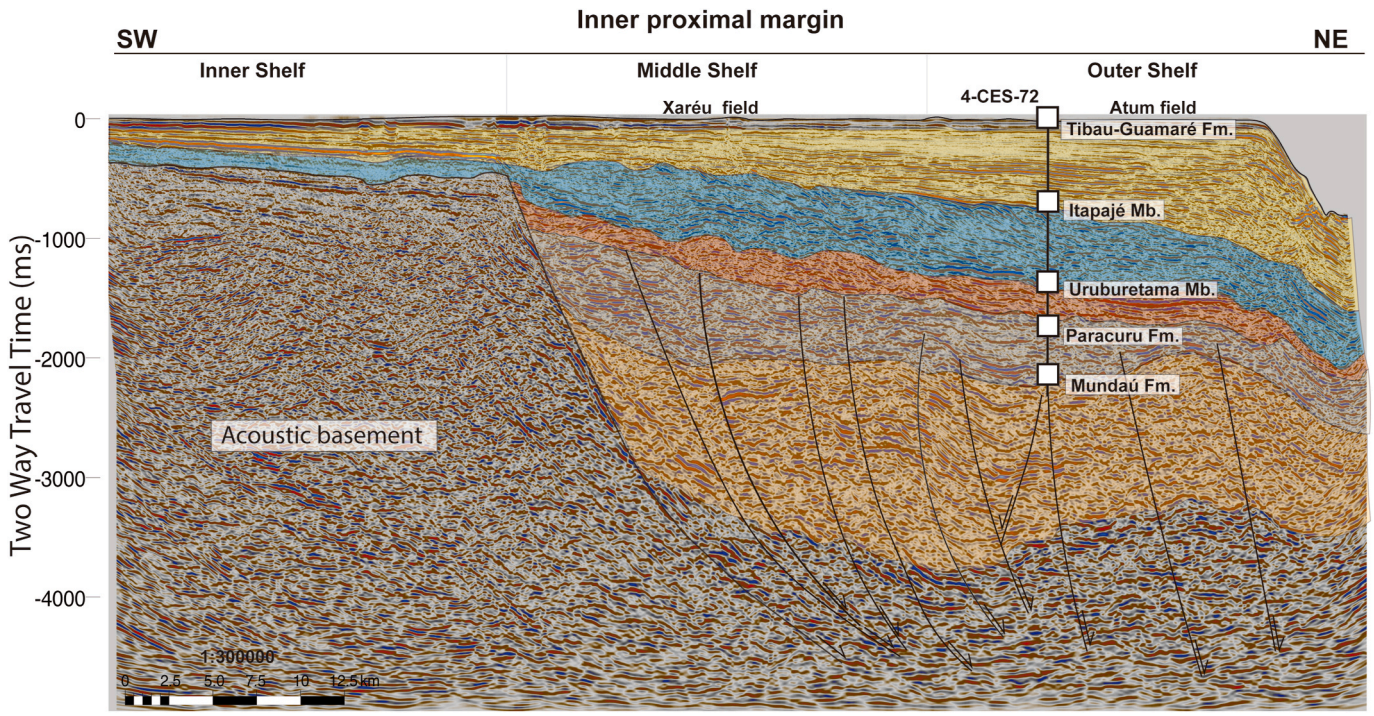

Fig. 4. Simplified interpretation of dip seismic reflection profile R0003 GRAND NORTH 0222 0506. MIG FIN.395 (For seismic profile location see Fig. 1C), showing the continuity of the Ceará Basin formations in the inner-, middle- and outer-shelf domains, as adopted in this paper for the study area.

dipping reflectors indicted the limit. In the middle shelf, chaotic reflections prevail, and in the inner shelf a prominent reflector separates the shallow basement from the parallel seismic reflector.

4.2.2. *Subunit 2 A – the base of the Mundaú Formation*

Subunit 2 A is the oldest stratigraphic layer of the Ceará Basin identified in the study area. This subunit is the thickest and has not been drilled. In the middle shelf, Subunit 2 A is limited by Horizon 1 (3500–4000 ms TWT) at the base and Horizon 2 (2000–2500 ms TWT) at the top. Subunit 2 A is characterized by a set of reflectors of high-intermediate continuity, with locally discontinuous, subparallel to wave internal reflection patterns, strong-moderate reflectors with stronger amplitude (Fig. 6). The continuity of the seismic reflectivity in Subunit 2 A generally decreases in the proximal domain close to the faults, which can be interpreted as syn-tectonic deposition. Subunit 2 A is interpreted as onlapping strata landward, limited by normal faults and downlapping in the reflector of basement forming occasional wedges composed of prograding reflectors in the rift sedimentary fill succession. The base of the Mundaú Formation is interpreted as a progradational seismic pattern. The pattern is discontinuous with onlapping and downlapping. Thickening of layers can be common in confined topography, associated with rapid changes in the depositional environment. This seismic facies suggests the presence of continental sedimentation associated with grabens and half-grabens during the early stages of the rifting event. Coarse-grained fluvial sediments, fine-grained sediments related to flood plains and lacustrine systems are associated with this event in a syn-depositional context.

4.2.3. *Subunit 2 B –The Mundaú Formation – transgressive sequence*

In general terms, Subunit 2 B shows parallel internal reflection patterns, strong amplitude seismic packages, mostly high frequency, and great lateral continuity. This subunit is limited by Horizons 2 and 3 (Fig. 6). The external geometry is sheet-like, whereas internal seismic reflectors consist of a set of parallel axes with concordant contacts. Thickness is relatively constant, despite faulting. Subunit 2 B is retrogradational on the coastal onlap landward and shows onlapping against the border fault. This is the most evident stacking pattern. The baselap (apparent onlap) surface is overlain by parallel to sub-parallel Subunit 2 A. This reflection can suggest that the depositional system formed under relatively stable and low-energy conditions. This interpretation is usually related to a transgressive systems tract. The top of Subunit 2 B limits the reflection-free (low reflectivity) seismic pattern that characterizes Subunit 2C.

4.2.4. *Subunit 2C – The Mundaú Formation – regressive sequence*

Subunit 2C, limited by Horizons 4 and 5, has a typically unclear or chaotic internal structure, although occasional steeply inclined or subparallel reflectors can be discerned. This subunit is dominated by relatively weak amplitudes throughout the entire sequence, in some parts being almost transparent. Continuous reflectors with low or poor continuity and internal pattern are reflection-free (low reflectivity). External structures present wedge-shaped features with downlapping reflectors. Subunit 2C is interpreted as oblique prograding in areas of high sediment supply – as base level rises, progradation occurs. Progradational reflectors show the progradation of the phase axis into the basin center, which is a common seismic reflection characteristic of the delta front facies; the transparent reflection represents deposition product with relatively high energy formed in turbulent hydrodynamic condition. An oblique geometry marks the external pattern and suggests little or no accommodation space during progradation. Infill associated with half grabens and faults limited the accommodation space. This subunit marks shifts from shoreline transgression to regression. At the base, downlaps divided subunits 2C and 2 B. Toplaps and truncations at the top are the patterns that indicate the limit of Subunit 2C.

4.2.5. *Subunit 2D – the top of the Mundaú Formation*

The last subunit of the Mundaú Formation is limited by horizons 5 and 6. Subunit 2D is characterized by high to intermediate reflection continuity (locally continuous), with internal sub-parallel patterns, and moderate to high frequency and strong amplitude. Two distinct external patterns are recognized in Subunit 2D. The first is wedge shaped and the stacking pattern of channels is related to regressive systems tracts. These

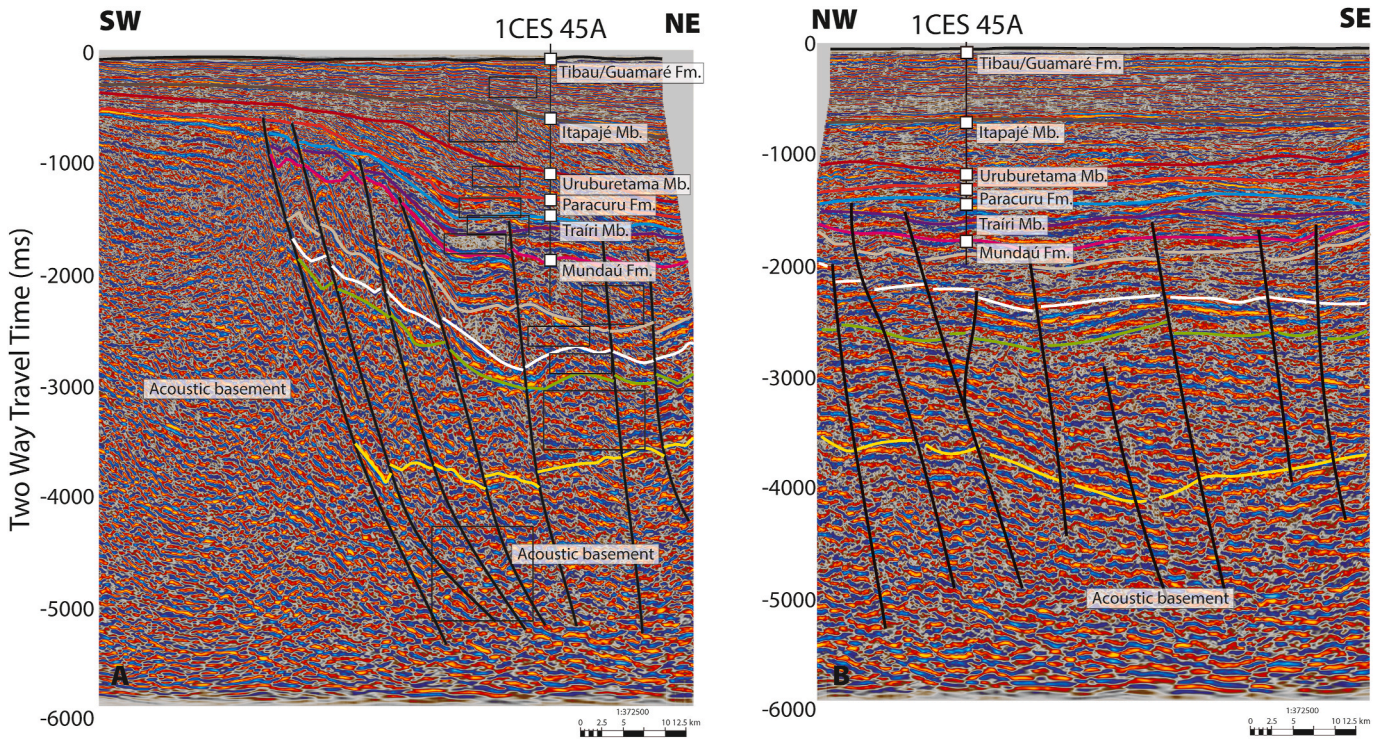

C

Unit	Seismic attributes	Seismic description: Frequency	Internal configuration	Continuity	Amplitude strength	Sequence attributes: External form	Stacking pattern	Internal termination	System tract	Interpretation	Depositional setting
Subunit 6	Horizon 11	Medium	Parallel	Continuous	Strong	Sheet or shingled	Aggradation and progradation	Onlap	Transgressive	Tibal and Gamaré Formations	Pelagic or hemipelagic
Subunit 5	Horizon 10	Medium to low	Divergent	Continuous	Moderate	Sigmoidal clinoforms	Progradational	Downlap, onlap and toplap	Regressive	Itapajé Member	Slop break deposits
Subunit 4	Horizon 9	High	Parallel to sub-parallel to locally wavy	Continuous	Moderate	Sheet to wedge	Retrogradational	Onlap and toplap or toplap truncation	Transgressive	Uruburetama Member	Shallow marine shelf
Subunit 3C	Horizon 8	Medium to high	Sub-parallel to concordant	High to medium or locally discontinuous	Moderate to strong	Oblique tangencial	Progradational	Downlap and toplap	Regressive	Top of Paracuru Formation	Shallow marine
Subunit 3B	Horizon 7	Medium	Sub-parallel	Semi-continuous to discontinuous	Strong to moderate	Sheet	Retrogradational	Onlap and concordant	Transgressive	Trairí Member	Lacustrine, deltaic and marine restrict deposits
Subunit 3A	Horizon 6	Low to high	Wavy to sub-parallel	Semi-continuous to continous	Weak to moderate	Assimetric wedge	Continuous Progradational	Angular truncation and downlap	Regressive	Base of Paracuru Formation	Turbidite and regressive sandstones
Subunit 2D	Horizon 5	Medium to high	Sub-parallel	Semi-continuous to locally discontinuous	Strong	Subparallel to sigmoidal	Continuous and Progradational	Downlap and angular truncation	Transgressive	Top of Mundaú Formation	Regressive system tract
Subunit 2C	Horizon 4	Low to medium	Sub-parallel to chaotic	Poorly - Continuous	Weak	Wedge convergent forming an oblique shape	Progradational	Downlap and toplap	Regressive	Deltaic front facies of Mundaú Fm.	High energy and turbulent conditions
Subunit 2B	Horizon 3	High	Parallel	Continuous	Strong	Sheet drape	Aggradational and retrogradational	Onlap landward	Transgressive	Transgressive mark of Mundaú Fm.	Relatively stable and low energy
Subunit 2A	Horizon 2	High to medium	Sub-parallel to wavy	Semi-continuous to continuous	Moderate	Wedge adjacent to border fault	Progradational	Onlap and downlap	Regressive	Base of Mundaú Formation	Continental sedimentation
Subunit 1	Horizon 1	Variable	Chaotic	Discontinuous	Weak to moderate	Highly disrupted	Chaotic	Chaotic	Absent	Basin acoustic basement	Non-stratified rocks

Fig. 5. Main seismic facies identified with 2D seismic profiling (For seismic profile location see Fig. 1C). A) Dip seismic line (0222 CEARÁ 6 B 0222 0529 MIG FIN 622) and the location of the subunits listed in C. B) Strike seismic line (0222 CEARÁ 6 B 0222 0554 MIG FIN 3) illustrating seismic characteristics of the subunits. C) Table showing the classification of seismic subunits based on the description of four seismic reflection attributes (frequency, internal reflection configurations, continuity and amplitude), four stratigraphic features (external forms, stacking pattern, internal termination and systems tract), interpretation and depositional environments. Identification and interpretation based on Vail (1977) and Veeken (2006).

tracts acted as by-pass channels, transporting sediments to deeper portions of the basin. Another possibility is that the turbidity currents no longer had enough energy to erode the underlying substrate, so that they deposited their sedimentary load.

The second pattern is positioned at the top and corresponds to the infilling of erosional features. It is characterized by seismic facies showing discontinuous, irregular, and strong-amplitude reflectors. These two external patterns are associated with a regressive to transgressive phase. Associated facies can be related to proximal siliciclastic and distal carbonate deposits, the latter expected to extend to the outer shelf and slope, below the zone of optimal carbonate production, as marls or siliciclastic mud.

The top of the Mundaú Formation is related to waning continental sedimentation and is characterized by an angular truncation that marks the erosional contact with the early sedimentation of the Paracuru Formation. The angular unconformity known as Electric Mark 100 is interpreted to be the last sequence boundary recognized in seismic and well-log data regarding the Mundaú Formation. The end of the continental interval presents rocks of the Mid-Aptian. The top of the Mundaú Formation is represented by a strong-amplitude and continuous reflector, which is also truncated and is overlain by a series of prograding reflections (Fig. 5D). Above the unconformity, three stratigraphic units are distinguished and related to the upper Albian to Aptian Paracuru Formation. Mark 100 represents a lithological change from sandstone and shale intercalations to siltstone, shale and carbonate deposits, and an environmental change from fluvial, floodplain to

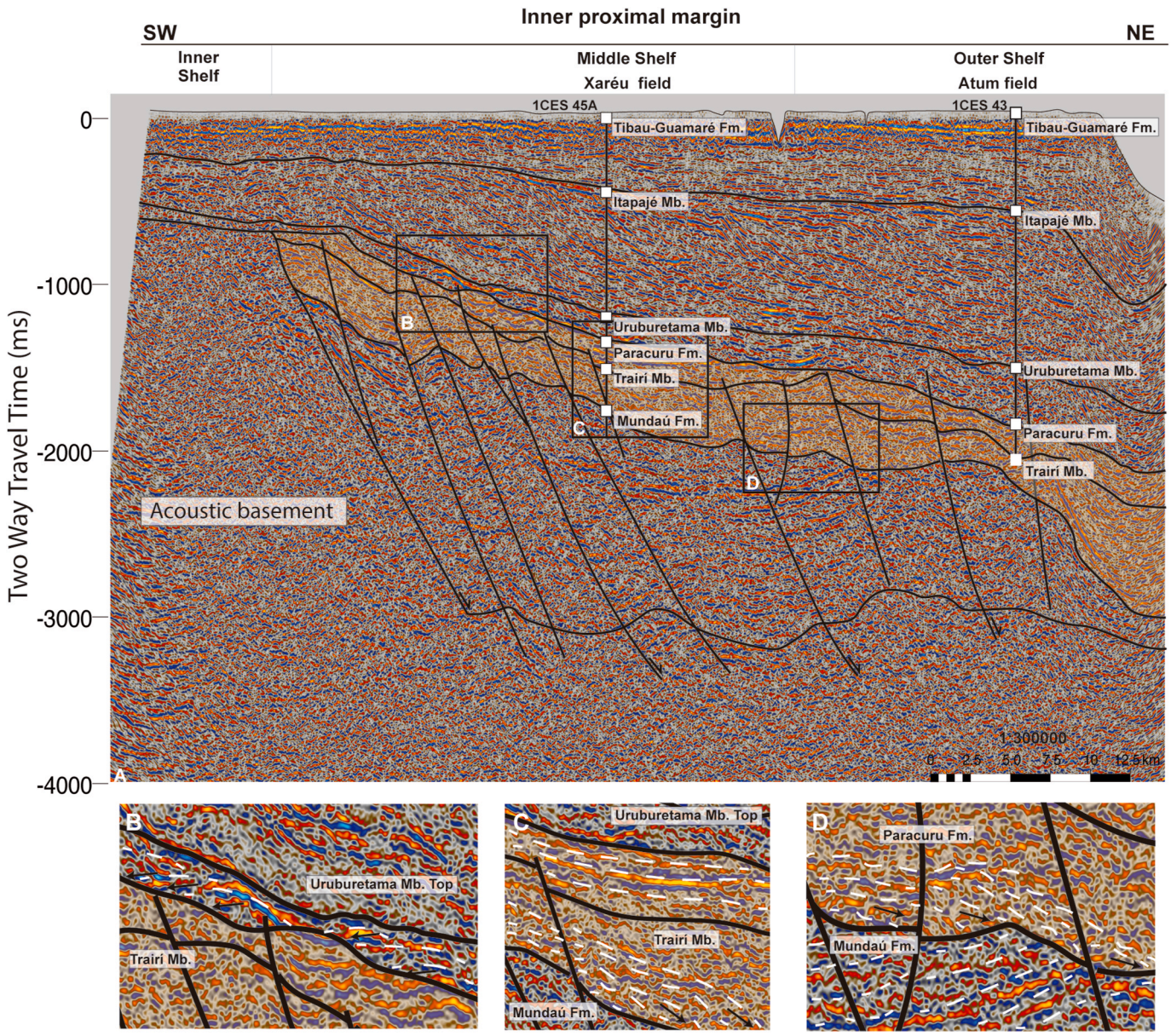

Fig. 6. Detailed dip seismic profiles (0047 CEARA 2 A.0047 0111. MIG FIN.2) across the Xaréu and Atum fields (For seismic profile location see Fig. 1C), highlighting the Paracuru Formation. A) Seismic record showing the base and top of the breakup sequence and tops of formations and members of the Ceará Basin. B) Interpretation of the stratigraphic framework of the Paracuru Formation top onlapped by the Uruburetama Member transgressive deposits (dashed white lines). C) Regional stratigraphic feature of the Trairí Member. Characterized by a strong-amplitude and continuous reflector, with downlap termination at the bottom and subparallel on top of this member (dashed white lines). D) Seismic interpretation of the base of the Paracuru Formation showing the truncation of rift sediments (dashed white lines below the arrows) and typical downlap geometries (dashed white lines above the arrows) formed by regressive systems tracts.

lacustrine systems, characterizing the transitional (rift to breakup) stage.

4.2.6. Subunit 3 A: the base of the Paracuru Formation

In seismic reflection profiles, the subunit 3 A, limited by horizons 6 and 7, is a strong marker and represents an erosional surface that defines a composite unconformity, which includes the sequence boundary previously described that separates the rift phase from the breakup sedimentation named Mark 100. Above the downlapping reflector of Subunit 2C, Subunit 3 A is identified as a chaotic reflector. The internal reflection pattern is subparallel, locally wave or transparent. Subunit 3 A is highly continuous. Inclined reflectors are associated with a series of moderate to high frequencies and weak to moderate amplitudes. This interval is made of turbiditic facies and in some cases regressive sand deposits. This deposition is caused by energy changes in the depositional environment in the middle shelf.

The recognition of seismic facies depends on and is associated with structural styles. For example, the basal sequence of the Paracuru Formation shows a complex downlapping wedge geometry that correlates with thicker sedimentation in proximal areas and listric faults. In distal areas, however, there is a decrease in the number of faults and change in inflection, which corresponds to parallel seismic facies deposited during seafloor spreading. The characterization of an extensional tectonics and diachronous breakup is attested by magmatic injections in deep-water regions (Maia de Almeida et al., 2020a; Leopoldino Oliveira et al., 2020). This magmatism allows to correlate the Paracuru basal sequence with the lithospheric breakup of the Equatorial Margin of Brazil from its counterpart in Africa, the Gulf of Guinea Province. Subunit 3 A also correlates with the Alagoas local stage (mid to late Aptian – see Fig. 2).

4.2.7. Subunit 3 B – the Trairí Member

Subunit 3 B is characterized by a concordant reflector of moderate to strong amplitude, limited by horizons 7 and 8. The internal reflection pattern is continuous, varying from wave to parallel and horizontal. The external geometry is sheet-like, whereas the internal seismic reflectors consist of a set of parallel axes with parallel contacts. The frequency and the amplitude are mostly high and strong to moderate, respectively. The reflectors form relatively thick packages, and, in some portions, they show wave to transparent internal pattern. The thickness is relatively constant. Such characteristics represent depositional systems formed under relatively stable and low energy conditions, as found in deep lacustrine environments.

The retrogradation pattern and erosional truncations at the top are associated with downlapping towards an unconformity that covers the overlying transgressive event interpreted as Subunit 3C. The gamma-ray pattern indicates finning upward of the sedimentary sequence, primarily consisting of shale, mudstone, carbonaceous mudstone and siltstone seams which act as seal or source rocks for the Ceará Basin petroleum systems. Sedimentation took place under steady and low-energy, subaqueous conditions, which denotes deep-lacustrine hydrocarbon source rocks. The external geometry is sheet-like, whereas the internal seismic reflectors consist of a set of parallel axes with parallel contacts. The thickness is relatively constant. Again, a depositional system formed under relatively stable and low-energy conditions, i.e. deep-lacustrine depositional environment, is indicated. The lithological change from sandstone to carbonate or restricted evaporites is the cause for the abrupt strong amplitude of this reflector. These isolated evaporitic layers are dated late Aptian to Mid Albian. In addition to the amplitude variability along the depositional dip, along-strike variations can also be expected, such as the presence of carbonate or hybrid deposits in areas of lower siliciclastic influx between deltaic systems. This interval is related to the Trairí Member deposited in restricted lacustrine, deltaic, and marine environments.

4.2.8. Subunit 3C – the top of the Paracuru Formation

The top of the Paracuru Formation comes after the top of the Trairí Member and extends to the beginning of the Uruburetama Member. This interval is limited by reflectors 8 and 9 and represents the end of the transitional sequence and the beginning of the drift sedimentation. The chronostratigraphic mark for this unit is the transition mid Albian-late Albian. The reflection patterns have moderate to strong amplitude with medium to high frequency. The internal geometry of the reflectors is sub-parallel to concordant and are of intermediate continuity and locally discontinuous. Subunit 3C is composed of oblique tangential clinoforms. Downlap and toplap characterize the lower and the upper boundaries, respectively. Lithological outstand over shale, limestone, mudstones eventually interlayered to sandstones. This subunit is interpreted as having a shallow marine signature. From base to top the subunits from Paracuru Formation are thinning.

4.2.9. Subunit 4 – the Uruburetama Member – transgressive sequence

Subunit 4, limited by horizons 9 and 10, corresponds to the Uruburetama Member and is characterized by onlap-type seismic reflection terminations indicative of transgression. The transgressive surface coincides with a regional unconformity, defined by toplap and/or toplap truncations. This reflector is of strong to moderate amplitude, mainly of high frequency and regional character. The internal reflection pattern is parallel-subparallel, locally wave, and continuity is high to intermediate and locally discontinuous. At the base, onlap and retrogradation patterns may indicate that the entry point of the sediment influx to the basin shifted landward or that the depocenters changed position, creating trough infill patterns. The parallel sub-horizontal seismic reflectors in the outer shelf are interpreted as shallow-marine deposits. A thin sequence that composes Subunit 4 is underlain by a downlap (Fig. 6B).

This reflection termination is interpreted as a transgressive marine sequence that presents retrogradational with a depositional surface moving landward and composed of shale or siltstone. The strong amplitude and continuous character of the reflector, its downlap pattern and the gamma-ray peak defining the top of the TST are all interpreted to represent the MFS at the top. This sequence correlates with the late Albian-Turonian. Sea-level rise builds the major marine transgressive systems tracts of the Ceará Basin. Downlap at the top is interpreted as corresponding to a sequence boundary represented by Horizon 10. Horizon 10 is the maximum flooding surface (MFS) forming the lower boundary surface of the following regressive systems tract.

4.2.10. Subunit 5 – The Itapajé Member – prograding sequence

Subunit 5 A is limited at the base by Horizon 10 and at the top by Horizon 11. The subunit contains an internal downlap surface, represented by stratified, semi-continuous reflections, indicating a dominantly hemipelagic deposition. This interpretation is supported by borehole information indicating a well-defined, continuous, and progradational and aggradational reflection pattern defined by overall constant thicknesses and parallel reflections, correlating with the Coniacian to Mid Eocene.

The regressive systems tracts are distinguished by progradational successions with internal clinoform geometry (sigmoid clinoforms). The Itapajé Member seismic mapping reveals thicker downlapping clinoforms in the distal area (Fig. 6C), identified in reflection records of the Atum field. In the Xaréu field the seismic termination is described as toplap or onlap of decreasing thickness. This description characterizes progradational clinoforms and supports the interpretation of regressive sequences for this member. The regressive interval is related to the advance of shelf slope break to basin landward. The deposition of sandstone and carbonate facies takes place at distal positions. This member comprises progradational parasequences. These sequences are further subdivided into three systems tracts with a predominant regressive interval dating Maastrichtian-Campanian. This prograding sequence is interpreted to constitute the RST that configures the top of Ubarana Formation.

4.2.11. Subunit 6 – the Tibal and Guamaré formations

Subunit 6 has continuous, parallel, and sub-horizontal to horizontal internal reflections, characterized by moderate to strong amplitude and moderate to high frequency. Subunit 6 is individualized by the onlapping that marks the sequence boundary and the top of the Itapajé Member (Horizon H11). The drill cores show seismic Subunit 6 consists primarily of shale interlayered with limestone, interpreted as hemipelagic to pelagic sediments. Previous studies have dated this subunit as Mid-Oligocene to recent. The lack of organic geochemical data is the reason why this subunit has not been included in the following sections.

4.3. Stratigraphic framework and organic geochemical data

The integration of gamma-ray data, seismic facies analysis, and organic geochemical data (TOC, GP, and RHP) results in the basis for interpretation of the transgressive-regressive (T-R) cycles. These results mark the time of transgression and regressions, which are functions of sea-level rises and falls. Transgressions are related to TOC preservation and consequently to anoxic events. Sea-level cycles comprehend relative sea-level maxima and minima and can be identified using fine-grained rocks, such as shales, because fine sediments are deposited in the early and late stages of these cycles (Figs. 7–10).

The Mundaú Formation is deposited as a 2nd order sequence (approximately 10–25 My) and is limited by faults and grabens toward the northeastern part of the study area. Electrical marks 70, 80, and 100 represent transgressive and regressive events that occurred in the Aptian (Condé et al., 2007). Mark 100 indicates the top of the last transgressive sequence and is interpreted as a sequence boundary for the overlying sedimentation. Six relatively short T-R cycles are interpreted in this study (Fig. 7). Well-log 1 CES 8 was initially considered the type of section of the Mundaú Formation by Beltrami (1994). Maximum

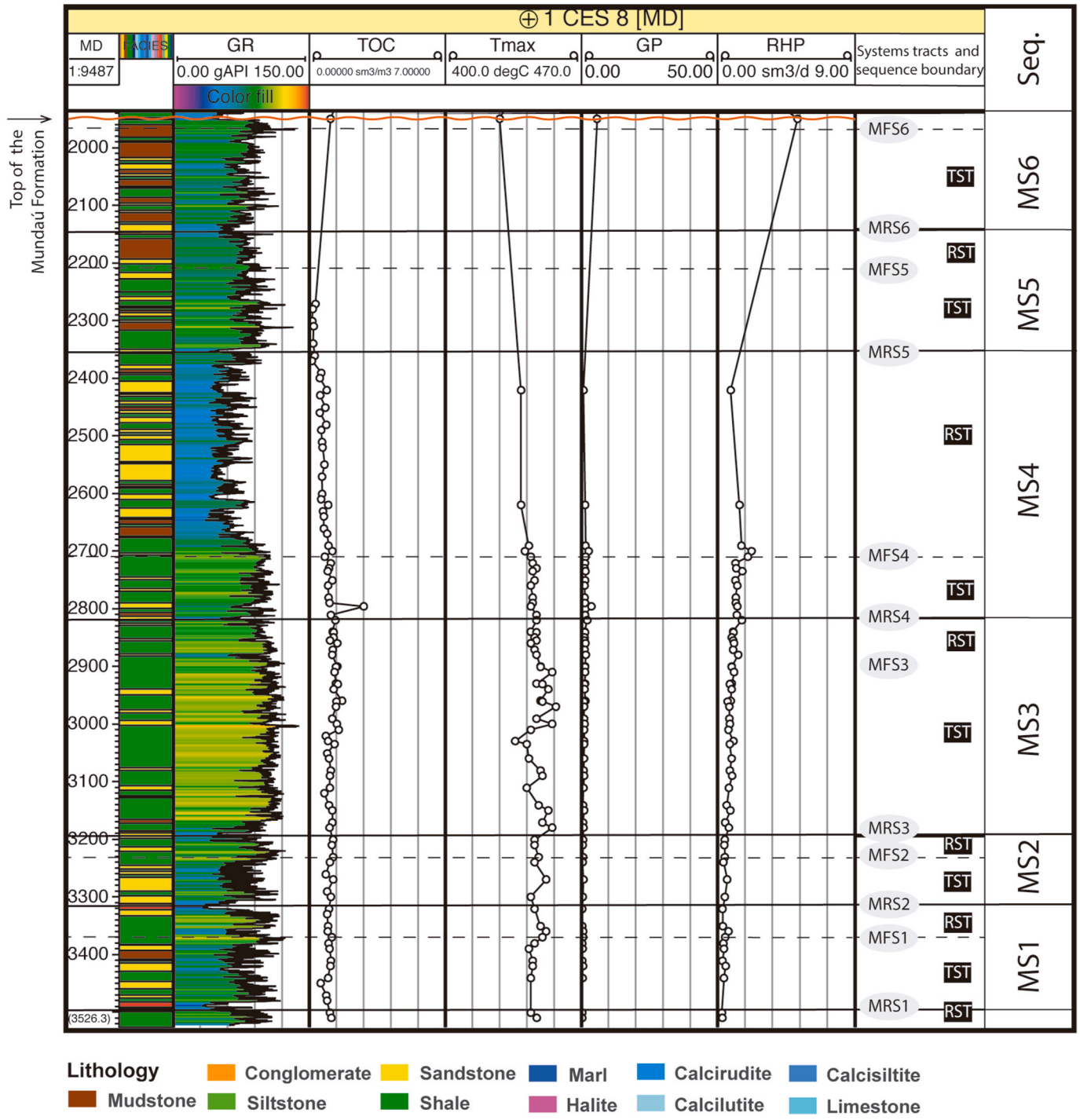

Fig. 7. Sequence-stratigraphic type section of the Mundaú Formation as described by Beltrami (1994), using well 1CES 8 and geochemical data including total organic carbon (TOC) trends along the depositional sequences. MRS = maximum regressive surface; MFS = maximum flooding surface; RST = regressive systems tract; TST = transgressive systems tract; MS = Mundaú sequence.

regressive surfaces (MRS) define the bases of T-R sequences MS1 and MS2 (Fig. 7) and are placed at gamma-ray minima and in the conglomerate facies. The bases of MS3, MS4, MS5, MS6 are also related to MRS placed in sandstone or siltstone, showing low gamma-ray and TOC values. Six transgressive systems tracts (TST) display upward-increasing gamma-ray values ("dirtying"). The maximum flooding surface (MFS) is placed at a gamma-ray peak (Fig. 7). The Mundaú Formation MFS reflects fining-up grain size and increasing TOC related to base level rising. In more distal areas, the first sequences have not been drilled and the top sequence seems to be very thin. In distal areas, TOC peaks are related to TST and spatially to border fault of field (See isoline maps of mean TOC values in Fig. 14A). At that time, environmental conditions were favorable to organic matter preservation under anoxic conditions, confirmed by Atum field well-log data. For the top of the Mundaú Formation, MFS is placed at a gamma-ray peak, a short distance above MRS. MFS is roughly coincident with a condensed section defined by thin shale layers. This interval is described as a hardground.

The Paracuru Formation was described using well-log 1 CES 80, positioned between the proximal and distal areas (Fig. 8). Well-log 1 CES

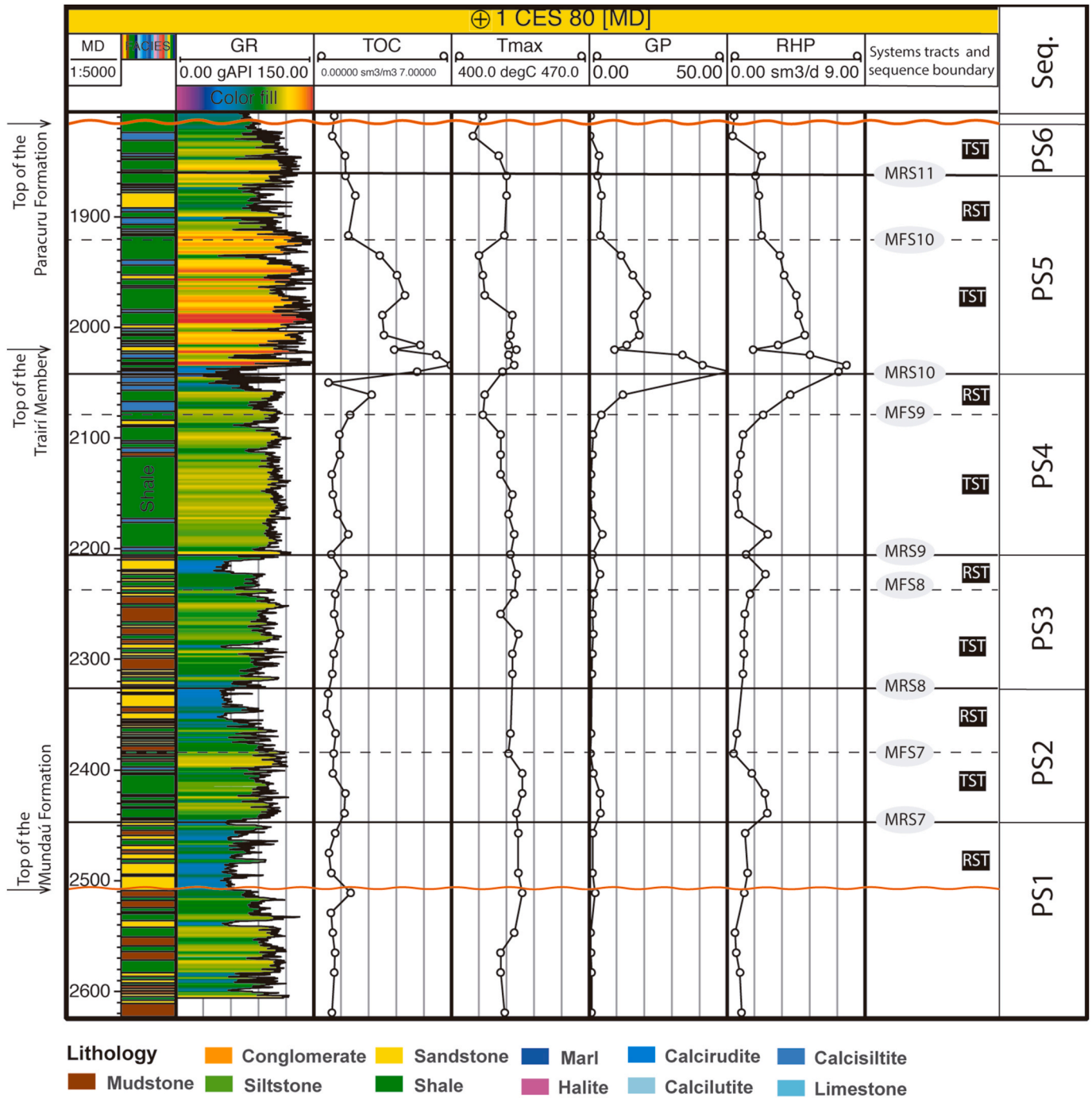

Fig. 8. Sequence-stratigraphic type section of the Paracuru Formation. The lower interval that encompasses the Trairí Member has been previously described as lower Paracuru sedimentation. The upper part of the Paracuru formation is related to late sedimentary sequences and encompasses the major geochemical marker of the Ceará Basin. TST = transgressive systems tract; RST = regressive systems tract; MFS = maximum flooding surface; MRS = maximum regressive surface; PS = Paracuru sequence.

6, type section of the Paracuru Formation (Betrami, 1994), was not available. Four complete T-R sequences were recognized. Paracuru Sequence 1 (PS1) is an incomplete sequence placed at a gamma-ray minimum close to or at the top of the Mundaú Formation. This interval is related to a regressive interval at the base of the Paracuru Formation, characterized by weak gamma-ray response, reduced organic carbon content and a sandstone facies. MRS-7 defines the base of a complete T-R sequence that begins with PS2. Both PS2 and PS3 are formed by shales or siltstones in a transgressive section and sandstones at the top of a regressive systems tract (RST). This intercalation is related to increasing clastic detritus deposition at proximal facies, were displaced seaward and accommodation space diminished. Beltrami (1994) and Condé et al. (2007) describe this interval as a main target for exploration. Costa et al. (1990), Condé et al. (2007), and Maia de Almeida (2020b) describe these facies as fluvial, deltaic, and lacustrine.

PS4 is the last sequence related to the lower Paracuru Formation. The observed base level fall reflects RST that finished at MRS-10 and culminated with the accumulation of carbonate and restricted halite deposits of the Trairí Member. This interval comprises a restricted environment that prograded in response to the base level fall. This

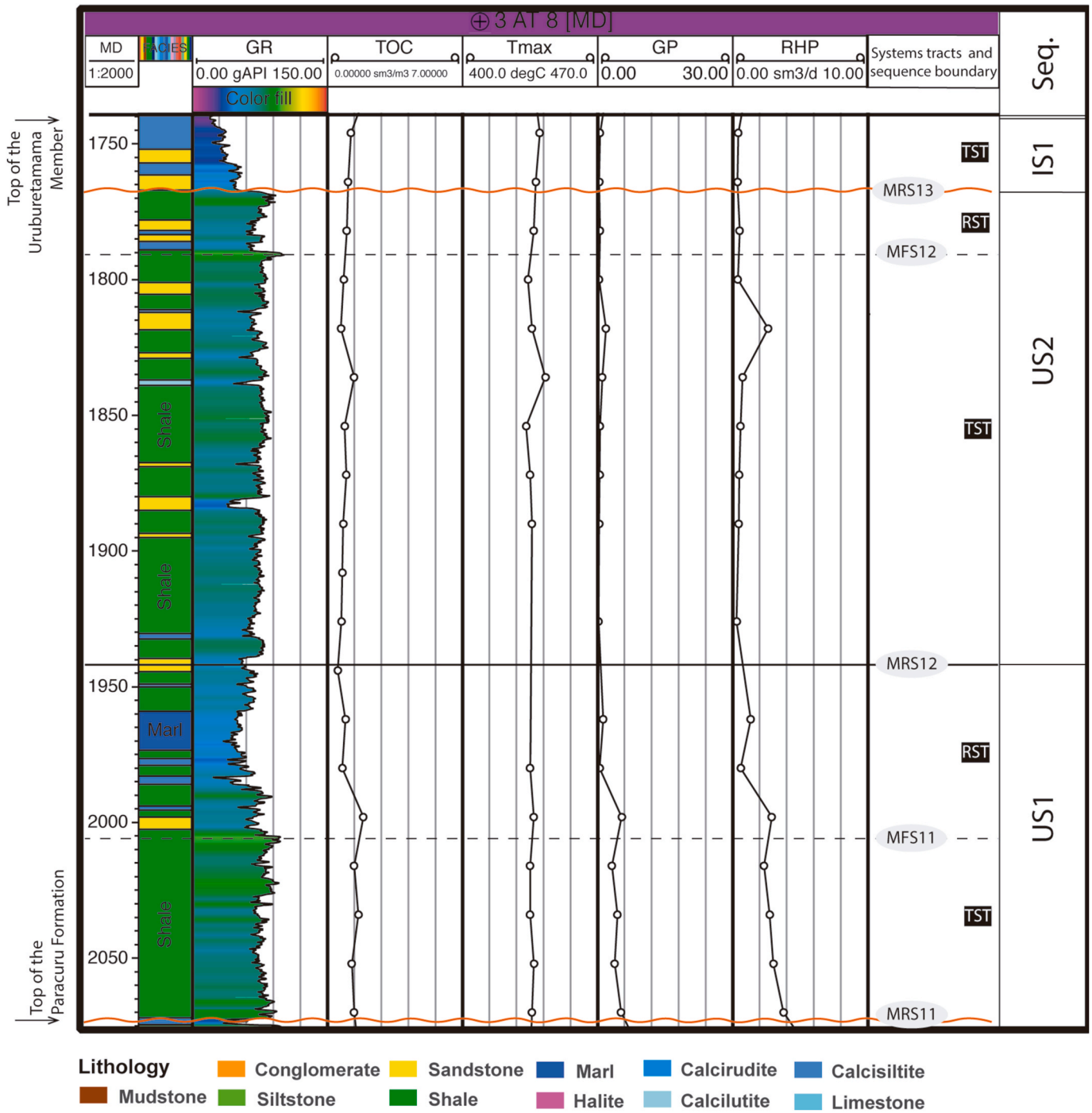

Fig. 9. Sequence-stratigraphic type section of the Ubarana Formation – Uruburetama Member. Note that the thickness of the transgressive interval is predominant (~50–150 m). TST = transgressive systems tract; RST = regressive systems tract; MFS = maximum flooding surface; MRS = maximum regressive surface. US = Uruburetama sequence.

stratigraphic interpretation supports the regressive phase observed in the geochemical dataset for the lower Paracuru Formation (Fig. 8) (see isoline maps of mean TOC values in Fig. 14B).

Regarding the upper Paracuru sedimentation, well-log signatures suggest a rapid transition from PS5, shown by high gamma-ray values, with asymmetric patterns typified by a rapid initial base level rise. TST in PS5 begins with carbonate deposition, which represents transgressive deposits and records the beginning of the PS5 base level rise. Shale and thin sandstone deposits at the top of this transgressive interval are formed close to MRS-10. The whole interval is marked by increases in organic carbon contents and gamma-ray intensity (see isoline maps of mean TOC values in Fig. 14C). These deposits comprise the bulk of a major TST. Geochemical data showed a strong correlation between maximum TOC values and intervals of sediment starvation. Sea environments, relatively high base levels and low sedimentation rate acted effectively to isolate shale and generate source rocks.

RST deposits immediately above MFS-10 (Fig. 8) record falling base levels, increasing sediment (sand) supply and consequently seaward shoreline shift. Increasing clastic detritus supply from the continent into the basin and consequent dilution of organic matter is reflected by diminishing TOC values. Furthermore, some gamma-ray logs display upward facies changes from lower organic carbon-rich RST layers to

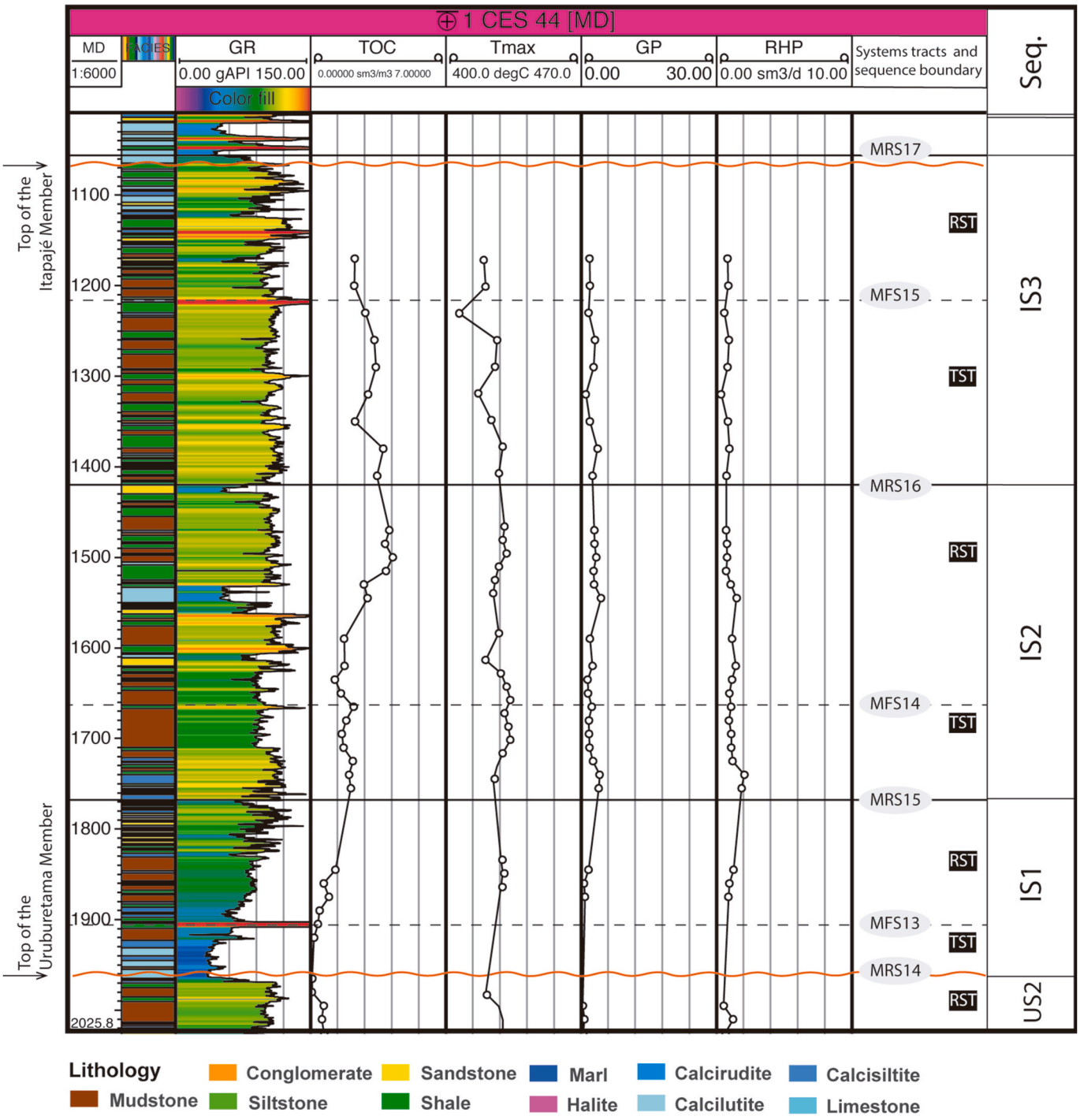

Fig. 10. Sequence-stratigraphic type section of the Ubarana Formation – Itapajé Member. Note that the thickness of regressive interval is predominant (~100–200 m). TST = transgressive systems tract; RST = regressive systems tract; MFS = maximum flooding surface; MRS = maximum regressive surface. IS = Itapajé sequence.

overlying organic carbon-poor RST layers.

Well-log 3 AT 8 was selected to represent the Uruburetama Member, as it is spatially near to well 1 CES 66, the type of section of this member (Fig. 9). The Uruburetama Member is in discordant contact with the Paracuru Formation, the contact separating a "dirtying-up trend" from an overlying "cleaning-up trend", which indicates a transgressive sequence (Emery and Myers, 1996). MRS-11 delimits the top of the Paracuru Formation. Carbonate accumulations occur at a gamma-ray minimum. Sequences US1 and US2 are dominated by a TST interval. Moreover, gamma-ray data suggest that transgressive systems tract deposits are less organic carbon rich than the Paracuru Formation.

The Uruburetama transgression is the largest of the drift phase from Ceará Basin, which can be visualized as a seismic facies retrogradation and attested by geochemical isoline maps of mean TOC values (see Fig. 14d). This interval is marked by landward onlapping TST deposits. US1 and US2 comprise the Uruburetama Member TST (Fig. 9). Rising base level is indicated by upward increasing gamma-ray response and increasing source rock potential. MFS is placed at the gamma-ray peak within the organic-rich layer and the best trend for other geochemical parameters. In the regressive event sandstones and marls are interlayered with shales and in the transgressive event thick shale layers predominate. Immediately overlying the RST deposits, a slow base level fall

and/or increased sediment influx relative to a base level rise is recorded, reflecting a decrease in organic carbon. The base level fall, attested by MFS-12 and MFS-13, culminates with the accumulation of carbonate interlayered with sand deposits during the early regressive sequence.

The Uruburetama Member includes facies deposited in fluvial and near-shore environments on the continental shelf. The beginning of the Uruburetama Member sedimentation is associated with the upper Aptian and extends to the Maastrichtian, which is marked by a regional regression and abrupt contact with the Itapajé Member.

The Itapajé Member begins with the regression that marks the Maastrichtian regional erosion. The type of section for this member is located in the Curimã field, outside the study area. Well-log 1 CES 44, located in a distal area, was selected because of the good geochemical and chronostratigraphic controls (Fig. 10). In distal areas, the Itapajé Member facies are fine grained, predominating calcitic shales, siltstones, and fine-grained sandstones interlayered with shales. Contrasting with relatively high TOC values in distal areas, the shales of the proximal areas are organic carbon-poor shales See isoline maps of mean TOC values in Fig. 14E).

The sequence-stratigraphic interpretation suggests a shoreline starting from a regressive seaward migration, shown in seismic data. RST is predominant in sequences IS1 and IS2. Increasing sediment supply results in progradation of coarser sediments across the shelf and siltstone predominance in distal areas. The surface defining the change from the transgressive systems tract to regressive systems tract is MFS (Embry et al., 2007; Embry, 2012). For this sequence, these surfaces are MFS15, MFS16, and MFS17. High TOC values found in thin shale beds are interpreted as condensed sections. In more basinal environments, this reflects the markedly reduced supply of clastic detritus ((Partington et al., 1993)). In some cases, such as IS2, the condensed section is close to or at the top of the transgressive systems tract. The described facies shift is manifested by a general upward increase in TOC from the base of the transgressive systems tract (Creaney and Passey, 1993). Still, organic-rich source rocks may continue to accumulate as part of the regressive systems tract as relative base level begins to fall. Further base level falling and reduction of accommodation space, however, is normally accompanied by an increase in clastic sediment influx and consequent dilution of organic matter (Creaney and Passey, 1993).

Despite well-log 1 CES 44 displays good TOC values locally, other essential parameters (e.g., temperature) makes this member less favorable for hydrocarbon generation. The evidence of high-energy media in proximal areas, the predominance of sandstones, the lack of geochemical data pointing to promising source rock potential, the progradation aspect in seismic data, the intercalation described as a turbiditic facies, suggest an oxic event for the Ceará Basin (Fig. 10).

4.4. Geochemical markers as indicators of sea-level fluctuations

The geochemical markers of the Mundaú Formation, the Paracuru Formation and the Uruburetama Member are related to maximum RHP values (anoxic conditions) (Fig. 11). Maximum RHP values correspond to maximum flooding surfaces (MFS), while minimum RHP values (oxic conditions) are associated with maximum regressive surfaces (MRS) (Figs. 11 and 12).

The Mundaú Formation was deposited over a time interval of approximately 10 My (125-115 Ma), which encompasses four 3rd order cycles from seismic interpretation (Fig. 5C). These T-R cycles are subdivided into six 4th order T-R cycles (Fig. 7). In the approach used here, the difference between long-term and short-term cycles occurs because of (i) variable thickness range of the drilled formations; and (ii) gap in some geochemical proxies (TOC, HI, and RHP). In Figs. 11 and 12, the top of the Mundaú Formation is marked by a TST and has a more organic-rich interval than the beginning of the formation, as evidenced by RHP values (see well logs 1 CES 8, 4 CES 13, 1 CES 80, and 1 CES 45 A). The upward increasing RHP values are related to kerogen type III instead of kerogen type IV, making this interval gas prone (Fig. 15). The terrestrial-derived organic matter is preserved during transgression and was transported basinward. A change in organic facies from hydrogen

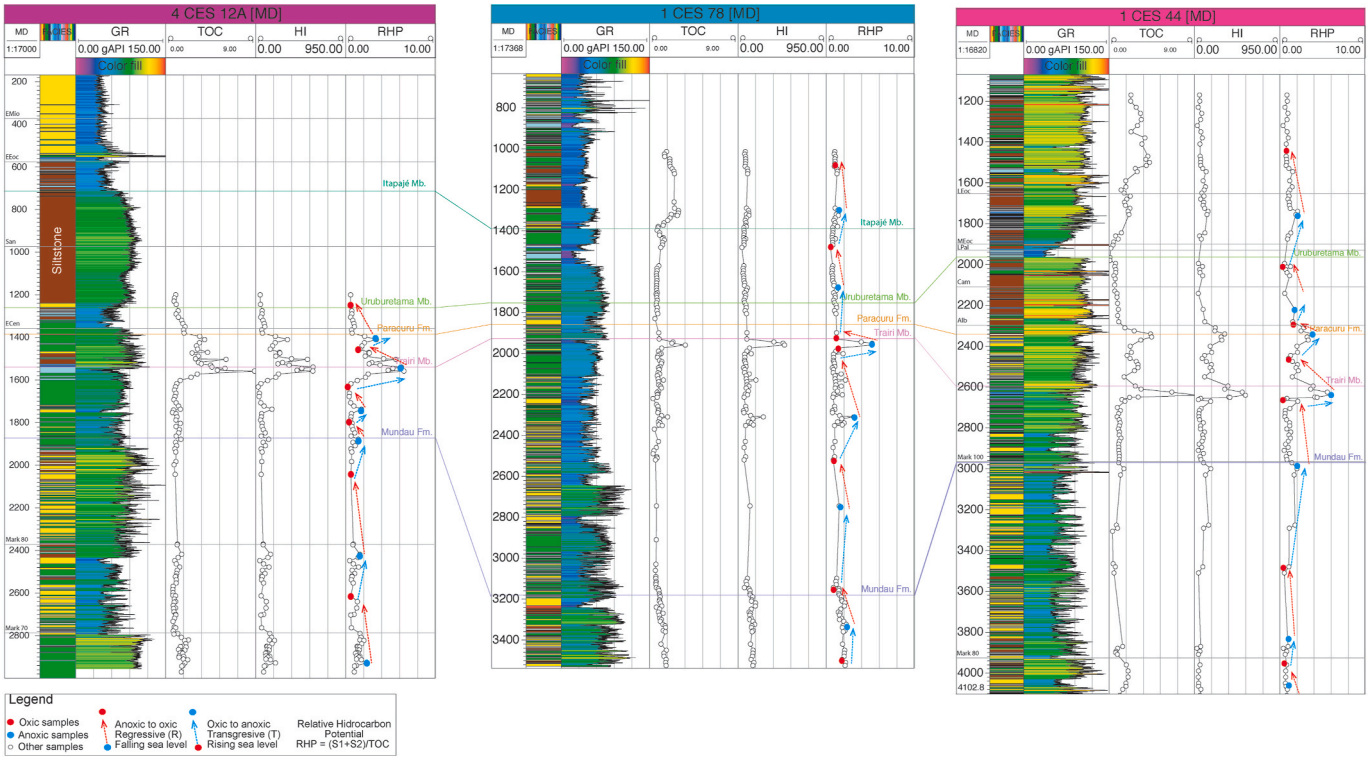

Fig. 11. Cross section correlations illustrating sea-level fluctuations indicated by hydrocarbon potential (RHP) values recorded in three well logs. The first well is located in the Xaréu field and the two others in the Atum field. Note the increasing RHP values (i.e., increasing anoxicity) at the base of the geochemical marker of the Paracuru Formation, implying sea-level rise or transgression.

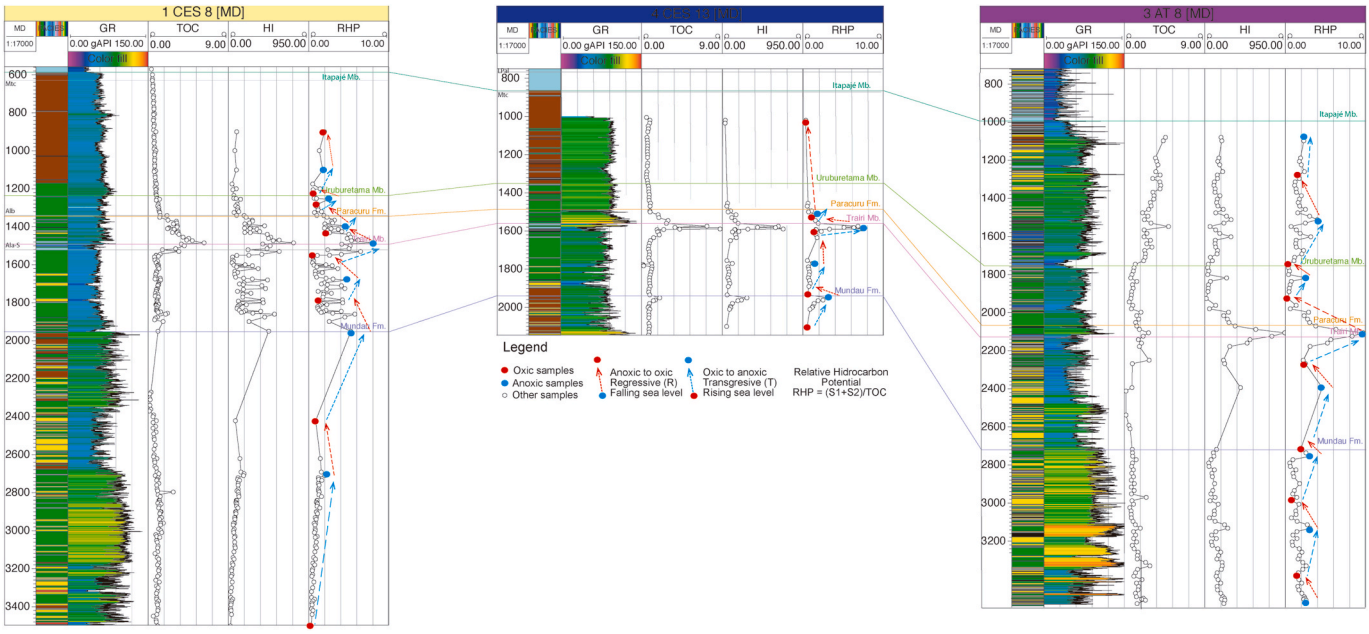

Fig. 12. Cross section correlations illustrating sea-level fluctuations indicated by hydrocarbon potential (RHP) values recorded in three well logs. The first and the second wells are located in the Xaréu field and third in the Atum field. Note the increasing RHP values (i.e., increasing anoxicity) at the base of the geochemical marker of the Paracuru Formation, implying sea-level rise or transgression.

poor to hydrogen rich from base to top, plus a related increase in RHP on top of the Mundaú Formation, indicates a change from oxic to anoxic conditions.

The Paracuru Formation was deposited over a time interval of approximately 5 My (115-110 Ma) which encompasses three 3rd order cycle from seismic interpretation (Fig. 5c). These T-R cycles are subdivided into six 4th order T-R cycles (Fig. 8). These six short-term T-R cycles are recognized within two long-term T-R cycles that collectively encompass the major geochemical marker of the Ceará basin, as discussed below. This initial deposition (lower Paracuru Formation) is related to the transition from continental to marine (first ingression) settings. The mixture of kerogen types in this stratigraphic unit indicates transitional environment (Souza et al., 2021). In this scenario, there is the predominance of transgressive events that reflect sea-level rising. The major geochemical marker is interpreted as having been generated in restricted marine conditions. The conditions are fundamental for the preservation of organic matter under anoxic conditions. The most expressive anoxic event of the Ceará basin is related to this time interval. After this interval, the last T-R cycle occurred, with the predominance of regressive events causing more oxygenation during sea-level falls. The abundant sediment supply under marine conditions makes this interval (upper Paracuru Formation). Both are the best source rocks for hydrocarbon generation (Fig. 15).

The deposition ages of the Uruburetama Member range from the Albian to the early Maastrichtian (110-70 Ma). In the Late Cretaceous, there was the predominance of marine facies related to the early drift stage. Tectonic activity, rapid production of oceanic crust and seamounts could play a fundamental role in global sea-level rising and subsequent transgression in northern Africa and probably in the Equatorial Margin during the upper Cretaceous (Bosellini et al., 1999; Adatte et al., 2002; Bachmann and Hirsch, 2006; Fluteau et al., 2007; Kidder and Worsley, 2010). The transgressions described in the Mundaú Formation, Paracuru Formation and Uruburetama Member correspond to thicker sequences and larger areas, when compared to those of the regressive phases. Biostratigraphic data attest that the Uruburetama transgression was a major event in the Ceará Basin (Lana et al., 2002). This significant transgression in the upper Cretaceous has been attributed to a global sea-level rise and represents the highest sea-level reached in the geological history (Haq et al., 1987, 2014).

The Itapajé Member was deposited from the early Maastrichtian to the Paleogene, for approximately 50 My (70-30 Ma). Regression is well represented in this unit. The progradation of facies is recorded in the Atum field (Figs. 11 and 12). In distal areas, the available geochemical indexes reveal changing conditions, but insufficient to promote hydrocarbon generation. In relation to sea-level fluctuation, the Itapajé Member was deposited during a 2nd order sea-level fall, represented by progradation clinoforms (downlap). Short-term superimposed 3rd order sequences consisting of three T-R cycles are overlain by the unconformable deposition of the Tibal and Guamaré formations.

4.5. *Stratigraphic correlations between the Ceará Basin geochemical markers*

Three sequence-stratigraphic cross sections reveal significant aspects of the Ceará Basin stratigraphic framework (Fig. 13). For the correlation, seismic facies, gamma-ray, TOC, HI and RHP data were used. The cross-section correlation (Fig. 13) shows gamma-ray peak, facies, and lateral correlation of the organic-rich intervals. Three geochemical markers are distinguished and there is a strong relationship between them and transgressive events and TOC contents.

The Mundaú geochemical marker is present in the proximal area of the Ceará Basin. This marker tends to intensify in middle areas. However, it was not identified in distal areas because of incomplete drilling. In middle areas this marker coincides with the top of the Mundaú Formation. RST deposited on top of the Mundaú Formation are suggestive of local erosion, causing the attenuation of this marker. The stratigraphic framework shows six relatively short-term, high-order T-R cycles that occurred from the Aptian to the Albian. However, using organic geochemical proxies, only two relatively long-term T-R cycles can be visualized during the deposition of this formation. The top of Mundaú is close to a transgression.

The major geochemical marker of the Ceará Basin is in the Paracuru Formation. This geochemical marker has a good lateral continuity, is identified in all well logs and is characterized by abrupt changes in TOC, HI, and RHP values (Fig. 11). It is associated with a TST located between the top of the Trairí Member and the upper Paracuru Formation.

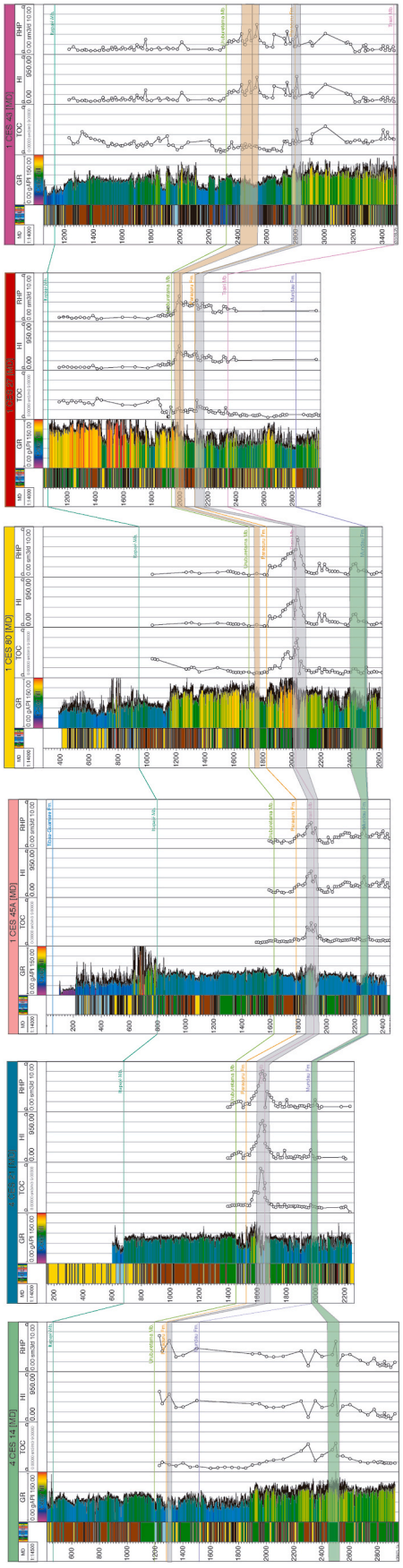

Fig. 13. Cross-section correlation illustrating lateral occurrence and thickness of the geochemical markers indicated by TOC, HI and RHP. The organic-rich intervals signal the markers. The major marker is associated with the top of the Trairí Member and the upper Paracuru Formation. Other markers are restricted to the top of the Mundaú Formation (proximal area) and to the base of the Uruburetama Member (distal area).

Previous paleoenvironmental interpretations indicate a marine setting for this interval. Most probably this marine setting could have supplied a high rate of organic matter for the basin. Therefore, this relationship justifies the presence of positive TOC values in this marker. Biostratigraphic studies (Lana et al., 2002) positioned the top of the Paracuru Formation in the Alagoas Stage. Additionally, this interval, in a global view, is related to an anoxic event.

The third geochemical marker detected in this study is related to the Uruburetama Member. Similarly, to the Mundaú Formation, this marker does not have a good lateral continuity and is related to transgressions. The Uruburetama Member was deposited under anoxic conditions and the Cenomanian-Turonian age is fundamental for the occurrence of this marker. In contrast, it is identified only in distal areas of the shelf. The presence of this marker is suggestive of organic matter deposition. As shown for the Paracuru Formation, the drift setting seems to be less favorable than the restricted marine conditions for hydrocarbon generation, as tectonic activity is weak or absent in drift sedimentation.

5. Discussion

5.1. Correlations between seismic sequence framework and TOC contents

Seismic data gives an indication of the spatial distribution of faults and sedimentation rates in a sedimentary basin. These approaches are important to discuss organic matter preservation, because two settings are possible. Frist, at low sedimentation rates, the lack of dilution by clastic sediments leads to high organic carbon contents. Second, at high sedimentation rates, high sediment supply rate can isolate organic matter from an oxidizing water and enhance organic-carbon content (Tayson, 2001). Besides, T-R cycles reflect the interplay between the creation or destruction of accommodation space and the rate of sedimentation, the controlling factors in basin infill dynamics irrespective of types of allogenic driving factors such as tectonics, eustasy, climate and geomorphology (Embry and Johannessen, 2017).

The geochemical markers of the Mundaú Formation TST include a condensed section (CS) and an MFS (Fig. 13). This interval presents high organic carbon contents (Figs. 11 and 12). The distribution and characteristics of the organic-rich strata are controlled from horsts and graben structures into tilted blocks (Fig. 14A). Their distribution and extension were previously described by Souza et al. (2021). In seismic profiles this configuration is characterized by thick progradational sections that comprise shale layers incorporated within limestone alternating with sandstone. TOC increase coincides with the transgressive systems tract (TST) near the Electrical Mark 100. This mark is interpreted to be the result of a period of regional flooding that affected the Ceará Basin during the lower Aptian (Pessoa Neto, 2004), and corresponds to a third-order sea-level fluctuation (Haq et al., 1987; Vail, 1977; Hardenbol et al., 1998).

The Paracuru Formation was deposited above Mark 100, shown by a retrogradational pattern with downlap following a progradational toplap (Figs. 5 and 6A). The base boundary is recognized by faulting and truncations, together with very large-scale unconformities. The regional seismic expression of the Paracuru Formation comprises high-to moderate-amplitude reflectors showing progradation towards the shelf edge. The progradational onlap is concordant with 3rd-order RST (Figs. 5 and 6). This progradation is related to a reduction in accommodation space due to a forced base-level fall or increasing sediment input. Both source rock and organic-rich facies also present progradational patterns (Fig. 14B), indicated by fining up (coarse-grained sediment deposition followed by shale or silt). This feature reflects tectonic evolution related to decrease in subsidence, despite such mechanism was an important post-rift tectonic activity that affected the tectonic and depositional evolution of the Ceará Basin.

The top of the Paracuru Formation present fine-grained rocks (shale or mudstone, siltstones) overlying carbonate successions. This facies combination can help absorb and bury organic matter (Bralower et al.,

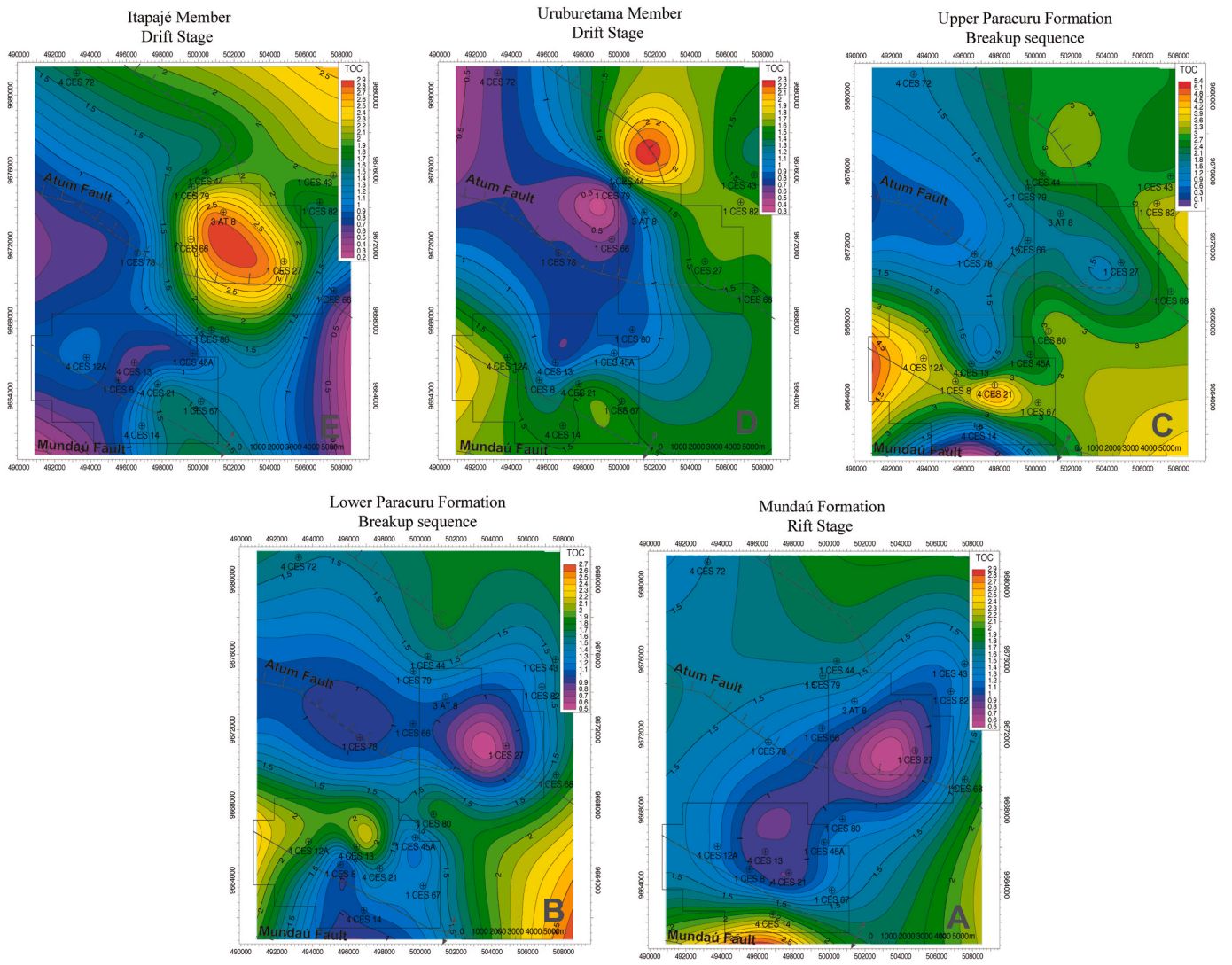

Fig. 14. Isoline maps of mean TOC values (wt. %) according to Souza et al. (2021). (A) Mundaú Formation; (B) Lower Paracuru Formation (interval between the top of the Mundaú Formation and the top of the Trairí Member); (C) Upper Paracuru Formation (interval between the top of the Trairí Member the top of the Paracuru Formation); (D) Ubarana Formation – Itapajé Member, and (E) Ubarana Formation – Uruburetama Member.

1999). Data point to sedimentation from continental to restricted marine environments (Condé et al., 2007). In this study, the TST close to TOC the top of the Trairí Member exhibits high organic carbon contents and high organic carbon. The TOC peak is related to widespread redox conditions (see next section). Organic matter preservation due to the rapid sea-level rise and transgression are proposed by Souza et al. (2021) (Fig. 14C). This interval is the major geochemical marker of the Ceará Basin and was favored by paleogeography and significant restricted paleoenvironment conditions, readily evolving from poorly oxygenated to anoxic conditions.

The Uruburetama Member transgressive systems tract (Fig. 6B and D) resulted from transgression with onlaps in proximal areas. It is subdivided in two T-R cycles, signaling the environmental change to marine and drift sedimentation (Costa et al., 1990; Condé et al., 2007). TOC distribution suggests that the organic-rich layers are restricted to intermediate deep waters (Fig. 14D). Vertical distribution of the source rocks in different localities depends on the position on the paleo-shelf/slope. The excellent TOC values indicate reducing marine conditions during transgression.

The Itapajé Member presents siltstones interbedded with mudstones, shales, limestones, and siltstones with interlaminated sandstones. It comprises a 3rd-order RST, which is further subdivided into a series of 4th-order progradational parasequences in response to rising sea-level. Accommodation increases less than sediment supply during sea-level fall. Facies transects may reflect a progressive increase in detrital material supply into the basin. Base-level fluctuations caused progradational migration of facies. Low TOC contents, low RHP values, the localization related to the outer shelf, and restricted area with source rock potential are explained by deposition under oxic conditions (Fig. 14E). The drift phase and water column reflect significant fluctuations in temperature, salinity, nutrients, and oxygen, unfavorable to source-rock generation.

5.2. *Tracking correlations with the Cretaceous Ocean Anoxic Events and implications for oil exploration*

The sedimentation in the Ceará Basin occurs from the Barremian to the recent (Condé et al., 2007; Leopoldino Oliveira et al., 2020). Globally, during this time interval six Ocean Anoxic Events (OAEs) have been identified: OAE-1A, OAE-1B, OAE-1D, OAE2, OAE3, and PETM (see Fig. 2 for the visualization of the OAEs that occur in the time interval of this study). These events are related to carbon cycle perturbations and are lithologically expressed by organic-rich levels (Jenkyns, 2010; Friedrich et al., 2012; Sabatino et al., 2015; Caetano-Filho et al., 2017;

Table 2
Comparison between source rocks of the Pará-Maranhão, Barreirinhas, Ceará, Potiguar and Gulf of Guinea Basins. Based on Trindade (1992), Brownfield and Charpentier (2006), Soares et al. (2007), Condé (2007); Pessoa Neto (2007); Trosdtorf Jr. et al. (2007), and Pellegrini and Ribeiro (2018).

Pará-Maranhão and Barreirinhas basins	Ceará Basin (this study)	Potiguar Basin	African basins (Some examples)	Paleoredox Conditions	Environment
No source rocks	Aptian lacustrine shales and siltstones Mundaú Fm.	Barremian to Aptian lacustrine shales Pendência Fm.	Neocomian Bucomazi Fm.; Congo Basin; oldest part of Ise Formation; Dahomey Basin	No Oceanic Anoxic Event	Lacustrine source rocks
Late Aptian to Lower Albian lagoon shales Codó Fm.	Late Albian to Aptian deltaic, lacustrine and restricted marine shales, siltstones, carbonates and halite Paracuru Fm.	Aptian Alagamar Fm.	No source rocks	Cretaceous Global Oceanic Anoxic Event correlated to OAE-1b	First marine transgressive event; extreme organic enrichment near evaporitic rocks
Late Albian to Early Cenomanian marine shales and calcilutites Caju Group	Late Albian to Early Cenomanian Uruburetma Mb.in continental shelf area	No source rocks	Late Albian marine shales Sekondi Fm. Keta Basin	Cretaceous Global Oceanic Anoxic Event correlated to OAE-1d	Marine transgressive event
Cenomanian-Turonian marine shales Travosas Fm.	Cenomanian-Turonian Uruburetma Mb in deep-water domain	No source rocks	Cenomanian-Turonian marine shales Awgu Fm. Benin Basin	Late Cenomanian Early Turonian Second Cretaceous Global Oceanic Anoxic Event (OAE-2)	Marine transgressive event
No source rocks	Campanian and Maastrichtian Sandstone interlayered with shale Itapajé Member	No source rocks	Campanian and Maastrichtian Araromi Fm. Dahomey Basin	Late Cenomanian Early Turonian Third Cretaceous Global Oceanic Anoxic Event (OAE-3) locally sub-oxic or oxic event	Marine regressive event sub-oxic or oxic expression

Bastos et al., 2020). The origin and preservation of organic-rich strata are distinguishing elements for potential source rocks and may reflect anoxic conditions in the water column. In a broad view, organic-rich rocks related to short-term global oceanic anoxic events, including OAE1a, OAE1b, and OAE2, have sourced almost one-third of the world's hydrocarbon reserves (Klemme and Ulmishek, 1991; Zobaa et al., 2011). In fact, these organic-rich sediments have large economic significance as they include more than 30% of the Aptian-Turonian reserves (ca. 125, 112, and 93.5 Ma), and 2% of the Coniacian–Santonian reserves (ca. 86 Ma). Oceanic anoxic events are reported in these periods (Schlanger and Jenkyns, 1976; Pedersen and Calvert, 1990; Wignall, 1991; Calvert et al., 1996; Nijenhuis et al., 1999; Lüning et al., 2004; Brumsack, 2006; Soua and Tribovillard, 2007; Jenkyns, 2010; Soua, 2014).

In the context of the Brazilian Equatorial Margin and its African counterpart, the Gulf of Guinea Basin, several offshore areas are bound to record these anoxic events along with their source-rock potential. These areas include the Pará-Maranhão, Barreirinhas, Ceará, and Potiguar basins in the Brazilian Equatorial Margin, and the Ivory Coast, Tano, Central, Saltpond, Keta, Benin, and Dahomey basins in the African Gulf of Guinea (Table 2). As main general features, these basins share a strike-slip tectonic style and absence of expressive evaporitic deposits. Additionally, the lack of long-lived deltaic systems in these areas would be a first argument in favor that high preserved organic matter contents are related to global anoxic events rather than local basin conditions (Brownfield and Charpentier, 2006; Pellegrini and Ribeiro, 2018). In this sense, anoxic events would be responsible for high hydrocarbon production potential. It must be stressed out that in general large deltaic systems lead to a rapid source-rock burial and high-quality hydrocarbon reservoirs.

As anoxic events have the potential to generate organic-rich strata, we will discuss the main features related to the source rocks of the Ceará Basin, as well as paleo-redox and paleogeographic conditions and comparisons between the Brazilian Equatorial Margin and its African counterpart.

The oldest source rocks of the Ceará Basin are lacustrine and deltaic shales of the Aptian Mandaú Formation. This interval is coeval with the Pendência Formation of the Potiguar Basin (Condé et al., 2007). Source rocks within this time interval were not found in the Pará-Maranhão and Barreirinhas basins (Pellegrini and Ribeiro, 2018). In the Gulf of Guinea, source rocks are identified in the Ise Formation of the Dahomey/Benin Basin (Brownfield and Charpentier, 2006). The Ise Formation contains conglomerates, sandstones, and shales that were deposited in continental and deltaic environments.

A TOC peak in the top of the Mundaú Formation sedimentary layers followed by a RHP increase (Fig. 14) is a geochemical marker related to transgressive systems tracts (TST) associated with the Electrical Mark 100. The shales of the Pendência Formation of the Potiguar Basin were deposited in a lacustrine depositional system and are thermally over-mature (Trindade et al., 1992; Pessoa Neto, 2007), similarly to the lower to mid Albian Mundaú Formation (Souza et al., 2021). Gas-prone source rocks have been identified in the Ivory Coast and Tano basins (Burke et al., 2003; Macgregor, 2010); in the Dahomey Embayment, in the Congo Basin (Tuttle et al., 1999; Haack et al., 2000; Kaki, 2013); in the Benue trough, and in the Keta and Ivory Coast basins. These source rocks are part of a sequence that consists of approximately 5000 m of Lower Cretaceous continental to marginal marine rocks deposited in grabens in the Ivory Coast and Tano basins (Chierici, 1996). Similar source rocks are likely to be present in the Keta and Benin basins. Geochemical and geological features similar to the Lower Cretaceous source rocks previously described are thick continental clastic sedimentation consisting of fluvial and possibly lacustrine facies, terrestrial signature and major gas potential (Fig. 16A).

In the Ceará Basin, these continental lacustrine source rocks have generated oil with high saturated hydrocarbon levels, low sulfur, and $\delta^{13}C < -28‰$, and comprise the Mundaú-Mundaú and Mundaú-Paracuru petroleum systems (Fig. 15). As seen before, the Mundaú Formation source rocks are gas-prone. The organic matter is of terrestrial origin (kerogen type III), was deposited in grabens during rift activity, and is thermally over-mature (Fig. 16A). The Aptian sequence of the Mundaú Formation is chrono-correlated with OAE-1a. However, its continental signature, highlighted by terrestrial input during transgressive phases does not support an association with this oceanic anoxic event.

The Paracuru Formation is upper Aptian to lower Albian in age. The paleoenvironment described for this breakup sequence includes deltaic and lacustrine sandstones, limestones and subordinate evaporites (Trairí Member) (Costa et al., 1990; Beltrami et al., 1994; Condé et al., 2007). Palynological interpretations suggest that this formation was coeval with the extinction of *Sergipea variverrucata* (palynozones P-270) and the

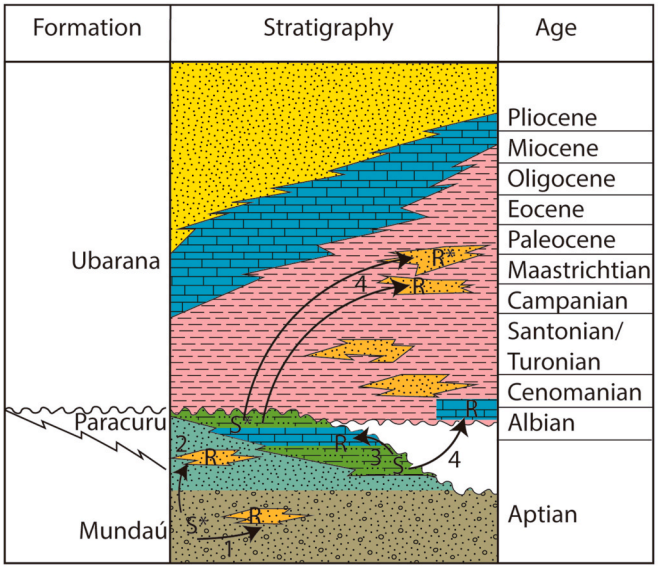

Fig. 15. Carbon isotopic data compiled from Rodrigues (1983), reinforcing the origin and migration of the accumulated hydrocarbons in the Ceará Basin. Petroleum accumulations occur in the same sequences that generate it (source rocks) or in overlying sequences. The 1) Mundaú--Mundaú, 2) Mundaú-Paracuru 3) Paracuru-Paracuru, 4) Paracuru-Ubarana petroleum systems are proposed by Rodrigues (1983), Costa et al. (1990), Pessoa Neto (2004), and ANP (2017) (see arrows maintaining the same numbering).

Formation	Well	Depth (m)	Carbon Isotope $\delta^{13}C$ (‰)	Tectonic context
Mundaú	1-CES-8	1702	-28.71	Rift
Mundaú	1-CES-8	1710	-28.71	Rift
Mundaú	4-CES-14	1255	-28.53	Rift
Mundaú	4-CES-14	1276	-28.53	Rift
Mundaú	4-CES-14	1578	-28.50	Rift
Mundaú	4-CES-14	1587	-28.50	Rift
Paracuru	1-CES-8	1475	-26.20	Breakup sequence
Paracuru	1-CES-8	1500	-26.20	Breakup sequence
Paracuru	1-CES-41	2674	-26.50	Breakup sequence
Paracuru	1-CES-41	2678	-26.50	Breakup sequence
Paracuru	1-CES-41	2725	-26.50	Breakup sequence
Paracuru	1-CES-41	2732	-26.50	Breakup sequence
Paracuru	3-CES-28	2044	-26.40	Breakup sequence
Paracuru	3-CES-28	2044	-26.40	Breakup sequence
Paracuru	1-CES-19	2121	-26.30	Breakup sequence
Paracuru	1-CES-19	2138	-26.30	Breakup sequence
Paracuru	4-CES-14	1578	-25,98	Breakup sequence
Paracuru	4-CES-14	1587	-25,98	Breakup sequence
Paracuru	4-CES-14	1001	-26.19	Breakup sequence
Paracuru	4-CES-14	1004	-26.19	Breakup sequence
Paracuru	l-CES-21	1310	-25,98	Breakup sequence
Paracuru	l-CES-21	1307	-25.98	Breakup sequence
Paracuru	4-CES-21	1307	-26.40	Breakup sequence
Paracuru	4-CES-21	1310	-26.40	Breakup sequence

first occurrence of *Complicatisacus cearenses* (palynozones P-280) (Regali, 1989). The extinction of *Sergipea variverrucata* occurred under extreme organic enrichment near the Trairí Member carbonates (Hashimoto et al., 1987; Regali, 1989). Similarly, to Bastos et al. (2020), this palynological argument was used to support an age correlation between the Paracuru Formation and the Santa Rosa Canyon section in Mexico (Bralower et al., 1999), where OAE-1b was described for the first time.

The sedimentary associations previously described support the existence of a restricted marine environment for the Paracuru Formation deposition (Hashimoto et al., 1987; Regali, 1989; Costa et al., 1990; Condé et al., 2007). This restricted setting was probably coeval with extremely hot climatic conditions. Globally, this warming is explained by high atmospheric CO_2 concentrations triggered by volcanic activity through periods of seafloor spreading (Arthur et al., 1985; Bice et al., 2006; Hofmann et al., 2008; Turgeon and Creaser, 2008). This hydrothermal volcanic influence may have played a role in oceanic water circulation (Hays and Pitman, 1973; Paytan et al., 2004), causing the warming of bottom waters of low circulation rates and less dissolved oxygen (Khalifa et al., 2018).

The anoxic bottom waters support organic-rich strata preservation for the Paracuru Formation and this interval may be related to the OAE-1b (Bralower and Thierstein, 1987; Wagner et al., 2007; Hofmann et al., 2008; Jenkyns, 2010; Friedrich et al., 2012; Sabatino et al., 2015; Caetano-Filho et al., 2017; Madhavaraju et al., 2018). The TOC peak near the top of the Trairí Member is an evidence of the occurrence of this anoxic event. The unusual TOC enrichment is recognized in all well logs of this study.

Additionally, stable isotopic data for the Paracuru Formation point to $\delta^{13}C$ close to −27‰ (Fig. 15). This value is comparable in magnitude to the $\delta^{13}C$ values obtained for the upper Aptian to lower Albian of the Codó Formation of the Parnaíba and São Luis basins (Bastos et al., 2020) and sections of the Araripe Basin from the Aptian-Albian transition (Benigno, 2019). These values are also similar to the classic isotopic records for the Aptian-Albian section of the Santa Rosa Canyon in Mexico (Bralower et al., 1999). All these organic-rich rocks are positioned in the OAE-1b event.

TOC increase, RHP increase and HI increase contents are related to transgressive events. The fluctuations in oxygenation conditions are reflected by variations in RHP, and maximum RHP values (anoxic conditions) correspond to flooding surfaces (MFS). Therefore, high organic matter contents in the Paracuru Formation were promoted by reduced terrigenous input during transgression phases, sea-level rise, spreading of source rock facies, as pointed out by Souza et al. (2021), and reduced tectonic activity and fault reactivation (Schlanger et al., 1987; Arthur and Sageman, 1994). These findings suggest that multiple causes, including sea-level changes, climatically-driven organic carbon burial, and structural framework contributed to the record of the Cretaceous OAE-1b.

Marine-evaporitic oils from the Alagamar Formation of the Potiguar basin have the same signature of those produced in the Paracuru Formation (see Cerqueira, 1985; Mello et al., 1988; Trindade et al., 1992; Santos Neto and Hayes, 1999). The source rocks of the Codó Formation present in both Pará-Maranhão and Barreirinhas basins originated under lagoon anoxic conditions in the Aptian, according to Soares et al. (2007) and Trosdtorf Jr. et al. (2007). This unit may be correlated with the source rocks from the late Albian, which are also present in the Gulf of Guinea basins (Brownfield and Charpentier 2006). The late Albian source rocks in the Ceará basin, that encompass the Paracuru-Paracuru and Paracuru-Urubarana petroleum system, basically consist of thermally mature, oil-prone, marine transgressive source rocks and marine evaporitic or mixed rocks, with predominating kerogen type III and minor types II and I (Fig. 16B).

The end of the syn-transform stage in the Gulf of Guinea and the end of the breakup sedimentation are delineated by a major unconformity, which separates it from the marine post-transform rocks of the uppermost Albian and Cenomanian (MacGregor et al., 2003). This unconformity is also readily recognized in the Brazilian marginal basins, which supports the interpretation that the two continents were close to one another during the Early Cretaceous and that their geological histories were similar during that time. Worldwide the Cenomanian-Turonian boundary is marked by the deposition of organic-rich shales that resulted from a period of increasing anoxia, due to the global anoxic events (Tissot et al., 1980; Soua and Tribovillard 2007; Jenkyns 2010; Rodrigues et al., 2019). This observation reinforces the interpretation of an anoxic event in the Ceará Basin and it correlates basins of the Brazilian and African margins.

According to Brownfield and Charpentier (2006), anoxic oceanic conditions that characterize the Middle Cretaceous and continued into the Turonian, affected the Gulf of Guinea resulting in the deposition of black shale source rocks in the Cenomanian-Turonian in the Ivory Coast and Tano basins. Samples analyzed from deep sea drilling sites both north and south of the Gulf of Guinea indicate that these source rocks contain more than 10% organic matter consisting of kerogen type II. According to Mello et al. (1988), the anoxic conditions also prevailed during most of the Cenomanian-Santonian interval in the Brazilian continental margin. The anoxic events in the Brazilian basins were intermittent, rather than continuous, covering relatively short periods of time, most of them associated with sea-level rises during transgression. These features fit to the sedimentary fill of Uruburetama Member. Leopoldino Oliveira et al. (2020) describe TOC values between 6 and 10 wt% in deep-water wells and Souza et al. (2021) describe the deposition under reducing conditions in a transgressive marine environment (Fig. 16C). The Cenomanian-Turonian black shales present on both Brazilian and African margins were deposited under anoxic conditions of the Second Cretaceous Global Oceanic Anoxic Event (OAE-2), characterized by periods of deposition of shale facies enriched in organic matter in almost every ocean of the world (Mello et al., 1988; Schiefelbein et al., 2000) (Table 2).

The Cenomanian-Turonian source rocks of the Uruburetama Member are described as transgressive marine shales, with oil-prone kerogen type II and II-III and terrestrial kerogen type III. This section is related to the Travosas Formation of the Pará-Maranhão and Barreirinhas basins. It is also correlated with marine black shales related to Cenomanian-Turonian anoxic events of the Gulf of Guinea basins. In the Potiguar basin, Cenomanian-Turonian sedimentation is related to high-energy carbonate source rocks of the Jandaíra Formation. In the Caju Group of the Potiguar, Pará-Maranhão and Barreirinhas basins, this interval is composed of shales and calcilutites deposited in a transgressive marine depositional environment according to Soares et al. (2007), Trosdtorf Jr. et al. (2007), Condé et al. (2007), and Pessoa Neto et al. (2007).

According to MacGregor et al. (2003) and Brownfield and Charpentier (2006), the most important source rocks within the Gulf of Guinea Province are Albian, Cenomanian, and Turonian marine shales, with oil-prone kerogen type II and II-III and terrestrial kerogen type III. These source rocks are distributed throughout the offshore part of the Gulf of Guinea Province and are expected to increase in thickness and quality into deep waters. Three main areas of hydrocarbon generation were interpreted by Chierici (1996) and MacGregor et al. (2003): the offshore of Ivory Coast and Tano basins; the offshore of Keta and Benin basins, and the Dahomey Embayment.

In comparison to the Brazilian Equatorial Margin, the lack of Maastrichtian and Campanian source rocks, e.g., in the Pará-Maranhão and Barreirinhas basins, can be discussed on the grounds of the importance of proximal extension in the tectonic evolution of the Equatorial Atlantic. Thus, crustal extension and restricted and anoxic conditions are preserved in portions between the Romanche Fracture Zone and the Chain Fracture. However, these conditions are lacking in eastern portion of this segment boundary by the St. Paul Fracture Zone and Romanche Fracture Zone.

When comparing the Araromi Formation developed during the drift stages of the Upper Cretaceous (Maastrichtian and Campanian) in the

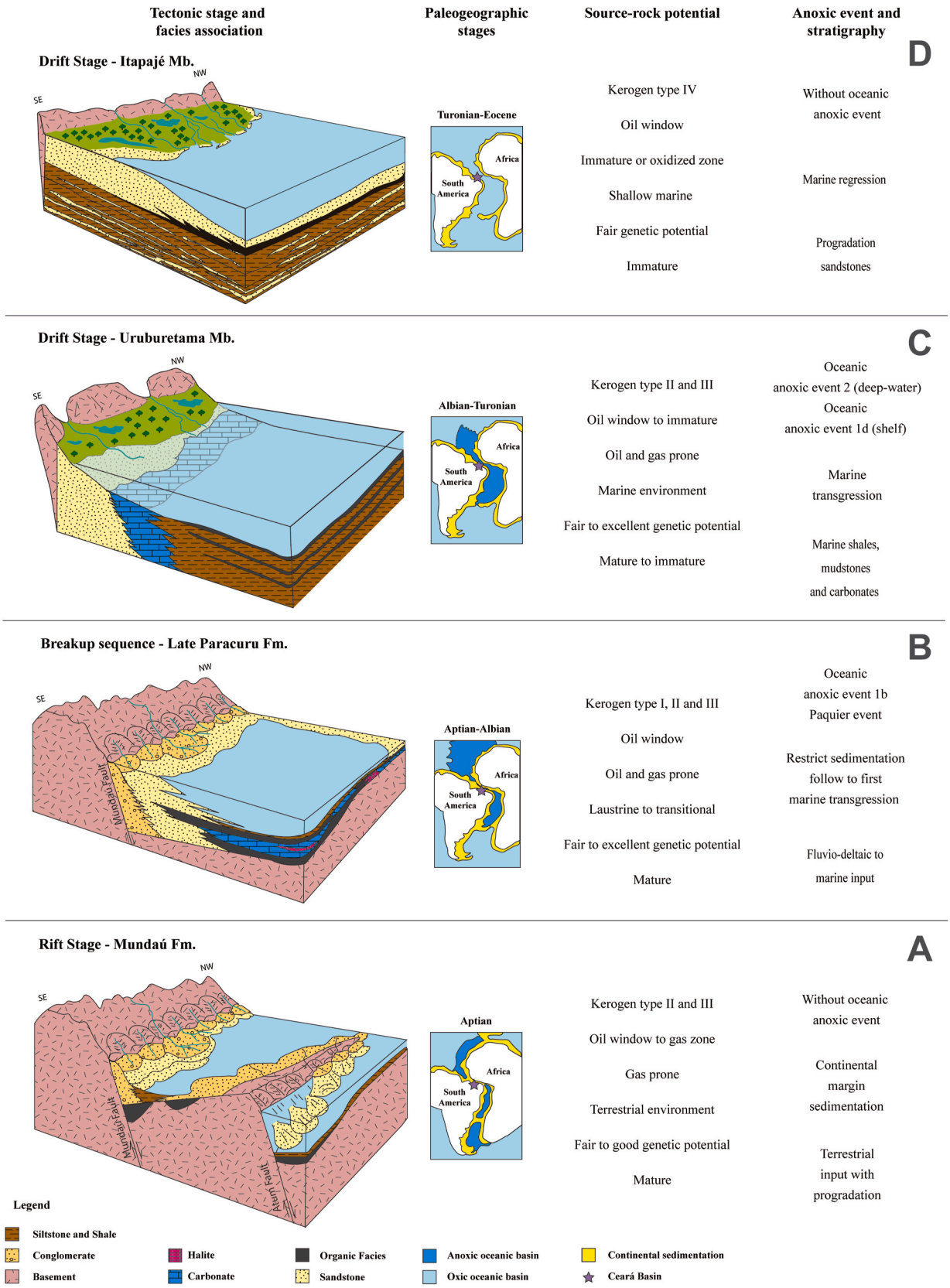

Fig. 16. Organic matter depositional model and its relationship with the Ceará Basin tectonic evolution. A) Rift stage – Mundaú Formation; B) Transitional stage/ Post-rift phase – Paracuru Formation; C) Transgressive drift stage – Uruburetama Member of the Ubarana Formation; D) Regressive drift stage – Itapajé Member of the Ubarana Formation. The tectonic stages are related to paleogeographic anoxic events in the Equatorial Margins of Africa and South America during the Cretaceous (modified from Tissot et al., 1980).

Dahomey basin, southwestern Nigeria, with the Itapajé Member, strong similarities are observed. Both contain kerogen type III and reworked organic matter (kerogen type IV), which probably resulted from the contribution of terrigenous components into the basin (Adekeye et al., 2019; Adeoye et al., 2020). The basal or deeper part of the wells is diagnostic of marine algal input, similar to the Itapajé Member (Fig. 16D). Organic constituents suggest more contributions from marine settings at the base of the wells, probably deposited under anoxic to sub-oxic conditions.

The source rocks are predominantly immature to marginally mature at shallow levels, particularly in the northern border of the Dahomey basin, but reaching proven maturity in the southern coastal and offshore areas, even though their potential source rocks are immature. The Araromi shales predominantly contain gas and exploration efforts should be targeted toward more promising, deeply buried source rocks, capable of generating hydrocarbons. This similarity attested the extension of oxidation that occurred in the Campanian and Maastrichtian.

6. Conclusions

This study evaluated the relationship between source rock potential and the sequence-stratigraphic interpretation of the Mundaú, Paracuru, and Ubarana formations of the Ceará Basin, in order to establish the origin and evolution of the organic matter, paleo-depositional environments, and paleogeographic setting from the Lower to Upper Cretaceous. The geochemical parameters helped identify anoxic events, sea-level changes, and R-T cycles in the Equatorial margins of Africa and South America during the Cretaceous.

For the Mundaú Formation, TOC, and other geochemical parameters suggested moderate to good source rock potential. Thermal maturity is high, and the source rocks are thermally mature to overmature, which indicates good potential for gas production. The source rocks capable of generating hydrocarbons are deeply buried. Intervals of high TOC values in proximal areas of the Mundaú Formation suggest high primary productivity. Lateral changes in the Mundaú Formation indicate increasing primary productivity coupled with increasing oxygen deficiency. These changes are related to border faults. Sediment supply during the rift phase points to favorable source rock generation. Kerogen types III and IV predominate. Type III kerogen and reworked organic matter in shallower parts of the Mundaú basin probably resulted from terrigenous contributions from the continent.

The top of the Mundaú Formation indicates that transgressive-regressive cycles occurred during the Aptian, being the main source-rock interval of this formation. Six T-R systems tracts are recognized along the type section (well-log 1 CES 8). Terrestrial-derived organic matter was preserved during the transgression event. From the relatively high source-rock and hydrocarbon potential, a proximal mark is interpreted as an anoxic period. This period is also recognized in the Pará-Maranhão, Barrerinhas, and Potiguar basins. In these basins, TOC contents increase upward, and the peak occurs in the lower part of the late rift section. The sedimentary influx is essential for deposition of organic matter and preservation.

Good to excellent source rocks are indicated for the Paracuru Formation. Kerogen type III predominates, with minor type II and I and mixed kerogen. The wide range of kerogen types indicates transitional environments. The organic-rick source rocks yielded a geochemical marker. This unit is thermally mature, and it is gas prone. Reduced tectonic events, the first marine ingression, indications of restricted environments may have promoted the significant petroleum potential.

The Paracuru Formation is the main oil source rock. The Aptian-Albian interval is a major regional geochemical marker. Six T-R systems tracts are interpreted, and the sedimentation is divided into the lower Paracuru Formation sedimentation, a regressive phase, and the lower Paracuru Formation sedimentation, a transgressive phase under marine and restricted conditions. Both conditions are essential for the preservation of organic matter in anoxic environments. This unit can be correlated with the source rocks of the late Albian-early Cenomanian of the Alagamar Formation and Caju Group of the Potiguar, Pará-Maranhão and Barreirinhas basins and with the Gulf of Guinea basins and the Benin Basin. This anoxic event recognized in the Ceará Basin and correlated basins is positioned in the first Global Oceanic Anoxic Event (OAE-1) of the Cretaceous.

The source rock potential of the Uruburetama Member varies from moderate to good and oil and gas prone. This unit is located in proximal areas of the Xaréu field and transgression events are interpreted to have favored reducing marine environments. The distal area related to the Atum filed is a little more promising and mixing of marine end terrestrial kerogen is assumed. This mixing is interpreted as relevant for TOC increase and probably this resulted from greater contribution from terrigenous components. T_{max} values point to immature to mature organic matter in proximal and distal areas, respectively. These results are more promising for samples falling in the oil window zone. The kerogen is type II, a mixture of type II and III, and minor type III.

Seismic data reveal transgression with onlaps in proximal areas of the Uruburetama Member. The systems tract is subdivided in two T-R sequences, predominating transgressive intervals. One geochemical marker is recognized in distal areas and in deep-water domine. The Uruburetama Member was deposited under anoxic conditions in the Cenomanian-Turonian. The Uruburetama Member drift sedimentation is recognized in other Equatorial margin source rocks, such as marine shales of the Travosas Formation and in African basins (Dahomey Basin, southwestern Nigeria belong to Ghana, Togo, and Benin). This interval formed during the Second Cretaceous Global Oceanic Anoxic Event (OAE-2).

The Itapajé Member presents low quality and quantity of organic matter mainly in proximal areas. TOC and S2 values suggest poor to fair source rock potential. Kerogen type IV was identified in the Xaréu field, and kerogen type IV and minor kerogen type III in the Atum field. Type IV is inert or degraded and type III is usually terrestrial. The presence of inert kerogen is related to high-energy depositional environments and oxic conditions. Terrestrial composition in distal areas corroborates the interpretation of a regressive event in the Ceará Basin. Source rocks are predominantly immature to marginally mature. These results indicate that the Itapajé Member may not have attained the required maturity to generate hydrocarbons.

The Itapajé Member regressive systems tract is composed of three T-R sequences, predominating regressive intervals. Progradation clinoforms and downlaps are interpreted in seismic profiles and in lateral well-log correlations. The comparison with other basins of the Equatorial margin shows that Maastrichtian and Campanian source rocks are lacking. In the African counterpart, the Araromi Formation is also interpreted as probably resulting from the contribution of terrigenous components under oxic to sub-oxic conditions.

Credit author statement

Ana Clara B. Souza: Conceptualization, data curation, investigation, formal analysis, visualization, writing - original draft, review and editing. **Daniel R. do Nascimento Jr**: Supervision. **Francisco Nepomuceno Filho**: Project administration, funding acquisition, resources, supervision. **Alessandro Batezelli**: Supervision. **Felipe H. dos Santos**: Visualization, writing - review and editing. **Karen M. Leopoldino Oliveira**: writing - review and editing. **Narelle Maia de Almeida**: writing - review and editing.

Declaration of competing interest

The authors declare that they have no known competing financial interests or personal relationships that could have appeared to influence the work reported in this paper.

Acknowledgements

We would like to thank the Brazilian National Agency of Petroleum, Natural Gas and Biofuels (ANP) for providing the seismic survey, well data, electrical logging and geochemistry data. We thank the Schlumberger for ceding the Petrel E&P software academic licenses. We thank the Federal University of Ceará (UFC) and Laboratory of Seismic Interpretation for institutional support. The first author thanks the Coordenação de Aperfeiçoamento de Pessoal de Nível Superior-Brazil (CAPES) - Finance Code 001 for granting the scholarship. We are grateful to Gianna M. Garda for her English proofreading. The authors also thank the editor and anonymous reviewers for the constructive recommendations that greatly improved this manuscript.

References

Abouelresh, M.O., Slatt, R.M., 2012. Lithofacies and sequence stratigraphy of the barnett shale in east-central fort Worth basin, Texas. Am. Assoc. Petrol. Geol. Bull. 96, 1–22. https://doi.org/10.1306/04261110116.

Adatte, T., Keller, G., Stinnesbeck, W., 2002. Late Cretaceous to early Paleocene climate and sea-level fluctuations; the Tunisian record.; Cretaceous-Paleogene transition in Tunisia, May 1998. Palaeogeogr. Palaeoclimatol. Palaeoecol. 178, 165–196.

Adekeye, O.A., Akande, S.O., Adeoye, J.A., 2019. The assessment of potential source rocks of Maastrichtian Araromi formation in Araromi and Gbekebo wells Dahomey Basin, southwestern Nigeria. Heliyon 5, e01561. https://doi.org/10.1016/j.heliyon.2019.e01561.

Adeoye, J.A., Akande, S.O., Adekeye, O.A., Sonibare, W.A., Ondrak, R., Dominik, W., Erdtmann, B.D., Neeka, J., 2020. Source rock maturity and petroleum generation in the Dahomey Basin SW Nigeria: insights from geologic and geochemical modelling. J. Petrol. Sci. Eng. 195, 107844. https://doi.org/10.1016/j.petrol.2020.107844.

Almeida, F.F.M., Brito Neves, B.B., Dal Ré Carneiro, C., 2000. The origin and evolution of the South American platform. Earth Sci. Rev. 50, 77–111. https://doi.org/10.1016/S0012-8252(99)00072-0.

Anders, D., 1991. Geochemical Exploration Methods: Chapter 7: Geochemical Methods and Exploration. Book Title: Source and Migration Processes and Evaluation Techniques, pp. 89–95. https://doi.org/10.1306/TrHbk543C7.

Anp, 2017. Bacia do Ceará - Sumário Geológico e Setores em Oferta 21.

Arthur, M., 1995. Marine shales: depositional mechanisms and environments of ancient deposits. Annu. Rev. Earth Planet Sci. 22, 499–551. https://doi.org/10.1146/annurev.earth.22.1.499.

Arthur, M.A., Sageman, B.B., 1994. Marine black shales: depositional mechanisms and environments of ancient deposits. Annu. Rev. Earth Planet Sci. 22 (1), 499–551.

Ashton, F., 2002. Transgressive-Regressive (T-R) Sequence Stratigraphy 151–172.

Azevedo, R.P., 1991. Interpretation of a deep seismic reflection profile in the Par'a-Maranhao Basin. In: Congresso Internacional da Sociedade Brasileira de Geofísica, vol. 2, pp. 661–666. https://doi.org/10.3997/2214-4609-pdb.316.122.

Bachmann, M., Hirsch, F., 2006. Lower Cretaceous carbonate platform of the eastern Levant (Galilee and the Golan Heights): stratigraphy and second-order sea-level change. Cretac. Res. 27 (4), 487–512. https://doi.org/10.1016/j.cretres.2005.09.003.

Barker, C., 1974. Pyrolysis techniques for source-rock evaluation. AAPG Bull. (American Assoc. Pet. Geol. 58, 2349–2361. https://doi.org/10.1306/83D91BAF-16C7-11D7-8645000102C1865D.

Bassiouni, Z., 1994. Theory, Measurement, and Interpretation of Well Logs Volumen 4.

Bastos, L.P.H., Pereira, E., da Costa Cavalcante, D., Ferreira Alferes, C.L., Jorge de Menezes, C., Rodrigues, R., 2020. Expression of Early Cretaceous global anoxic events in Northeastern Brazilian basins. Cretac. Res. 110 https://doi.org/10.1016/j.cretres.2020.104390.

Beers, R.F., 1945. Radioactivity and organic content of some Paleozoic shales. AAPG (Am. Assoc. Pet. Geol.) Bull. 29, 1–22.

Behar, F., Beaumont, V., De, B., Penteado, H.L., 2001. Rock-eval 6 technology: performances and developments. Oil Gas Sci. Technol. 56, 111–134. https://doi.org/10.2516/ogst:2001013.

Beltrami, C.V., Alves, L.E.M., Feij'o, F.J., 1994. Bacia do Ceará. Boletim de. Geoci. Petrobr'as 8, 117–125.

Benigno, A.P.A., Saraiva, A.Á., Sial, A.N., Lacerda, L.D., 2020. Mercury chemostratigraphy as a proxy of volcanic-driven environmental changes in the Aptian-Albian transition, Araripe Basin, northeastern Brazil. J. S. Am. Earth Sci. 103020.

Bice, K.L., Birgel, D., Meyers, P.A., Dahl, K.A., Hinrichs, K.U., Norris, R.D., 2006. A multiple proxy and model study of Cretaceous upper ocean temperatures and atmospheric CO2 concentrations. Paleoceanography 21 (2).

Bohacs, K.M., Carroll, A.R., Neal, J.E., Mankiewicz, P.J., 2000. Lake-basin type, source potential, and hydrocar-bon character: an integrated-sequence-stratigraphic–geochemical framework. In: Gierlowski-Kordesch, inE.H., Kelts, K.R. (Eds.), Lake Basins Throughspace and Time, vol. 46. AAPG Studies in Geology, pp. 3–34.

Bosellini, A., Russo, A., Schroeder, R., 1999. Stratigraphic evidence for an early aptian Sea-level fluctuation: the graua limestone of south-eastern Ethiopia. Cretac. Res. 20 (6), 783–791. https://doi.org/10.1006/cres.1999.0183.

Bralower, T.J., Thierstein, H.R., 1987. Organic carbon and metal accumulation rates in Holocene and mid-Cretaceous sediments: palaeoceanographic significance. Geol. Soc. Lond. Spec. Publ. 26 (1), 345–369.

Bralower, T.J., Arthur, M.A., Leckie, R.M., Sliter, W.V., Allard, D.J., Schlanger, S.O., 1994. Timing and paleoceanography of oceanic dysoxia/anoxia in the late Barremian to early Aptian (early Cretaceous). Palaios 9, 335–369. https://doi.org/10.2307/3515055.

Bralower, T.J., Cobabe, E., Clement, B., Sliter, W.V., Osburn, C.L., Longoria, J., 1999. The record of global change in mid-Cretaceous (Barremian-Albian) sections from the Sierra Madre, Northeastern Mexico. J. Foraminifer. Res. 29, 418–437.

Brownfield, M.E., Charpentier, R.E., 2006. Geology and Total Petroleum Systems of the Gulf of Guinea Province of West Africa, vol. 32. USGS Bull.

Brumsack, H.J., 2006. The trace metal content of recent organic carbon-rich sediments: implications for Cretaceous black shale formation. Palaeogeogr. Palaeoclimatol. Palaeoecol. 232 (2–4), 344–361.

Buckner, N., Slatt, R.M., Coffey, B., Davis, R.J., 2009. Stratigraphy of the Woodford Shale from Behind-Outcrop Drilling, Logging, and Coring. AAPG Search and Discovery Article, p. 50147.

Burke, K., Macgregor, D., Cameron, N., 2003. African petroleum systems: four tectonic "aces" in the past 600 million years. In: Arthur, T.J., Macgregor, D.S., Cameron, N.R. (Eds.), Petroleum Geology of Africa: New Themes and Developing Technologies. Geological Society [London] Special Publication 207, pp. 21–60.

Caetano-Filho, S., Dias-Brito, D., Rodrigues, R., de Azevedo, R.L.M., 2017. Carbonate microfacies and chemostratigraphy of a late Aptian–early Albian marine distal section from the primitive South Atlantic (SE Brazilian continental margin): record of global ocean-climate changes? Cretac. Res. 74, 23–44.

Calvert, S.E., Bustin, R.M., Ingall, E.D., 1996. Influence of water column anoxia and sediment supply on the burial and preservation of organic carbon in marine shales. Geochem. Cosmochim. Acta 60 (9), 1577–1593.

Catuneanu, O., 2019. Scale in sequence stratigraphy. Mar. Petrol. Geol. 106, 128–159. https://doi.org/10.1016/j.marpetgeo.2019.04.026.

Catuneanu, O., Abreu, V., Bhattacharya, J.P., Blum, M.D., Dalrymple, R.W., Eriksson, P. G., Fielding, C.R., Fisher, W.L., Galloway, W.E., Gibling, M.R., Giles, K.A., Holbrook, J.M., Jordan, R., Kendall, C.G.S.C., Macurda, B., Martinsen, O.J., Miall, A. D., Neal, J.E., Nummedal, D., Pomar, L., Posamentier, H.W., Pratt, B.R., Sarg, J.F., Shanley, K.W., Steel, R.J., Strasser, A., Tucker, M.E., Winker, C., 2009. Towards the standardization of sequence stratigraphy. Earth Sci. Rev. 92, 1–33. https://doi.org/10.1016/j.earscirev.2008.10.003.

Catuneanu, O., Galloway, W.E., Kendall, C.G.S.C., Miall, A.D., Posamentier, H.W., Strasser, A., Tucker, M.E., 2011. Sequence stratigraphy: methodology and nomenclature. Newslett. Stratigr. 44, 173–245. https://doi.org/10.1127/0078-0421/2011/0011.

Cerqueira, J.R., Soldan, A.L., Mello, M.R., Beltrami, C.V., 1994. Identificacao das Rochas Geradoras de Hidrocarbonetos da Bacia do Cear'a. XXXIII Congresso. Brasileiro de Geoleologia. Cond'e, V.C., Lana.

Chierici, M.A., 1996. Stratigraphy, palaeoenvironments and geological evolution of the ivory coast-Ghana basin. Bull. Cent. Rech. Explor.-Prod. Elf-Aquitaine - Mem. 16, 293–303.

Condé, V.C., Lana, C.C., Da Cruz Pessoa Neto, O., Roesner, E.H., De Morais Neto, J.M., Dutra, D.C., 2007. Bacia do Ceará. Bol. Geociencias Petrobras 15, 347–355.

Costa, I.G., Beltrami, C.V., e Alves, L.E.M., 1990. A Evolução Tectono-Sedimentar e o Habitat do Óleo da Bacia do Ceará. Bol. Geoci. Petrobras Geoci. PETROBRÁS 4, 65–74.

Creaney, S., Passey Q. R., Recurring patterns of total organic carbon and source rock quality within a sequence stratigraphic framework. AAPG (Am. Assoc. Pet. Geol.) Bull., 77, 386-401.

Curiale, J.A., 2017. Total Organic Carbon (TOC) 1–5. https://doi.org/10.1007/978-3-319-02330-43-1.

Daher, B.S., Nader, F.H., Müller, C., Littke, R., 2015. Geochemical and petrographic characterization of Campanian-Lower Maastrichtian calcareous petroleum source rocks of Hasbayya, South Lebanon. Mar. Petrol. Geol. 64, 304–323. https://doi.org/10.1016/j.marpetgeo.2015.03.009.

Davison, I., Faull, T., Greenhalgh, J., O Beirne, E., Steel, I., 2016. Transpressional structures and hydrocarbon potential along the Romanche Fracture Zone: a review. Geol. Soc. London, Spec. Publ. 431, 235–248. https://doi.org/10.1144/sp431.2.

Dean, W.E., Arthur, M.A., 1989. Fe-S-C relatiohship in organic carbon rich sequences. Am. J. Sci. https://doi.org/10.2475/ajs.289.6.708.

Delgado, L., Batezelli, A., Luna, J., 2018. Journal of south American earth sciences petroleum geochemical characterization of albian-oligocene sequences in the campos Basin : " case study : eastern marlim oilfield , offshore , Brazil. J. South Am. Earth Sci. 88, 715–735. https://doi.org/10.1016/j.jsames.2018.10.009.

Demaison, G.J., Moore, G.T., 1980. Anoxic environments and oil source bed genesis. Org. Geochem. 2, 9–31. https://doi.org/10.1016/0146-6380(80)90017-0.

Dembicki, H., 2009. Three common source rock evaluation errors made by geologists during prospect or play appraisals. Am. Assoc. Petrol. Geol. Bull. 93, 341–356. https://doi.org/10.1306/10230808076.

Embry, A.F., 2012. Transgressive-regressive (T-R) sequence stratigraphy. Seq. In: Stratigr. Model. Explor. Prod. Evol. 1563 Methodol. Emerg. Model. Appl. Hist. 22nd Annu., pp. 151–172. https://doi.org/10.5724/gcs.02.22.0151.

Embry, A.F., Johannessen, E.P., 1993. T–R sequence stratigraphy, facies analysis and reservoir distribution in the uppermost Triassic–Lower Jurassic succession, western Sverdrup Basin, Arctic Canada. In: Norwegian Petroleum Society Special Publications. Elsevier, pp. 121–146.

Embry, A.F., Johannessen, E.P., 2017. Two approaches to sequence stratigraphy. https://doi.org/10.1016/bs.sats.2017.08.001 https://doi.org/10.1139/e93-024, 2-85-118.

Embry, A., Johannessen, E., Owen, D., Beauchamp, B., 2007. Sequence Stratigraphy as a " Concrete " Stratigraphic Discipline Report of the ISSC Task Group on Sequence Stratigraphy 104.
Emery, D., Myers, K. (Eds.), 2009. Sequence Stratigraphy. John Wiley & Sons.
Espitalié, J., MarquisF, I.B., 1984. Geochemical Logging, Geologic Log Interpretation. Butterworth & Co (Publishers) Ltd. https://doi.org/10.2110/scn.94.29.0135.
Espitalie, J., Madec, M., Tissot, B., Mennig, J.J., Leplat, P., 1977. Source rock characterization method for petroleum exploration. Proc. Annu. Offshore Technol. Conf. 1977-May 439–444. https://doi.org/10.4043/2935-ms.
Fang, H., Jianyu, C., Yongchuan, S., Yaozong, L., 1993. Application of organic facies studies to sedimentary basin analysis: a case study from the Yitong Graben. China. Org. Geochem. 20, 27–42. https://doi.org/10.1016/0146-6380(93)90078-P.
Fang, H., Zhou, X., Zhu, Y., Yang, Y., 2011. Lacustrine source rock deposition in response to co-evolution of environments and organisms controlled by tectonic subsidence and climate, Bohai Bay Basin. China. Org. Geochem. 42, 323–339. https://doi.org/10.1016/j.org geochem.2011.01.010.
Fluteau, F., Ramstein, G., Besse, J., Guiraud, R., Masse, J.P., 2007. Impacts of palaeogeography and sea level changes on Mid-Cretaceous climate. Palaeogeogr. Palaeoclimatol. Palaeoecol. 247 (3–4), 357–381. https://doi.org/10.1016/j.palaeo.2006.11.016.
Freire, A.F.M., Monteiro, M.C., 2013. A novel approach for inferring the proportion of terrestrial organic matter input to marine sediments on the basis of TOC:TN and $\delta^{13}C_{org}$ signatures. Open J. Mar. Sci. 3, 74–92. https://doi.org/10.4236/ojms.2013.32009.
Friedrich, O., Norris, R.D., Erbacher, J., 2012. Evolution of middle to Late Cretaceous oceansda 55 my record of Earth's temperature and carbon cycle. Geology 40 (2), 107e110.
Gambacorta, G., Bottini, C., Brumsack, H.J., Schnetger, B., Erba, E., 2020. Major and trace element characterization of oceanic anoxic event 1d (OAE 1d): insight from the umbria-marche basin. central Italy. Chem. Geol. 557, 119834. https://doi.org/10.1016/j.chemgeo.2020.119834.
Gröcke, D.R., Hesselbo, S.P., Jenkyns, H.C., 1999. Carbon-isotope composition of Lower Cretaceous fossil wood: ocean-atmosphere chemistry and relation to sea-level change. Geology 27, 155–158. https://doi.org/10.1130/0091-7613(1999)027.
Gürgey, K., Bati, Z., 2018. Palynological and petroleum geochemical assessment of the lower oligocene mezardere formation, thrace basin, NW Turkey. Turk. J. Earth Sci. 27, 349–383. https://doi.org/10.3906/yer-1710-24.
Haack, R.C., Sundararaman, P., Diedjomahor, J.O., Xiao, H., Gant, N.J., May, E.D., Kelsch, K., 2000. AAPG Memoir 73, vol. 16. Niger Delta Petroleum Systems, Nigeria.
Hancock, J.M., Kauffman, E.G., 1979. The great transgressions of the Late Cretaceous. J. Geol. Soc. London. 136, 175–186. https://doi.org/10.1144/gsjgs.136.2.0175.
Haq, B.U., 2014. Cretaceous eustasy revisited. Global Planet. Change 113, 44–58. https://doi.org/10.1016/j.gloplacha.2013.12.007.
Haq, B.U., Hardenbol, J., Vail, P.R., 1987. Chronology of fluctuating sea levels since the Triassic. Science 235 (4793), 1156–1167. https://doi.org/10.1126/science.235.4793.1156.
Harbor, R.L., 2011. Facies Characterization and Stratigraphic Architecture of Organic-Rich Mudrocks. Upper Cretaceous Eagle Ford Formation, South Texas. Thesis 184pp.
Hardenbol, J.A.N., Thierry, J., Farley, M.B., Jacquin, T., De Graciansky, P.C., Vail, P.R., 1998. Mesozoic and Cenozoic Sequence Chronostratigraphic Framework of European Basins.
Harris, N.B., Freeman, K.H., Pancost, R.D., White, T.S., Mitchell, G.D., 2004. The character and origin of lacustrine source rocks in the Lower Cretaceous synrift section, Congo Basin, west Africa. Am. Assoc. Petrol. Geol. Bull. 88, 1163–1184. https://doi.org/10.1306/02260403069.
Hart, G., 1994. Maceral palynofacies of the Louisiana deltaic plain in terms of organic constituents and hydrocarbon potential. In: Traverse, A. (Ed.), i>Sedimentation of Organic Particles. Cambridge University Press, Cambridge, pp. 141–176. https://doi.org/10.1017/CBO9780511524875.010.
Hart, B.S., Steen, A.S., 2015. Programmed Pyrolysis (Rock-Eval) Data and Shale Paleoenvironmental Analyses: A Review. Interpretation 3, SH41–SH58. https://doi.org/10.1190/INT-2014-0168.1.
Hashimoto, A.T., Appi, C.J., Soldan, A.L., Cerqueira, J.R., 1987. The Neo-Alagoas in the Ceara, Araripe and Potiguar basins (Brazil): stratigraphic and paleoecological characterization. Rev. Bras. Geociencias 17, 118–122.
Hays, J.D., Pitman, W.C., 1973. Lithospheric plate motion, sea level changes and climatic and ecological consequences. Nature 246 (5427), 18–22.
Heine, C., Brune, S., 2014. Oblique rifting of the equatorial atlantic: why there is no saharan atlantic ocean. Geology 42, 211–214. https://doi.org/10.1130/G35082.1.
Heine, C., Zoethout, J., Müller, R.D., 2013. Kinematics of the south atlantic rift. Solid Earth 4, 215–253. https://doi.org/10.5194/se-4-215-2013.
Hesselbo, S.P., 1996. Spectral gamma-ray logs in relation to clay mineralogy and sequence stratigraphy , cenozoic of the atlantic margin , offshore New Jersey 1 Relationship of Spectral Gamma-ray Units to Depositional Geometry. Proc. Ocean Drill. Progam, Sci. Res. 150, 411–422.
Hofmann, P., Stüsser, I., Wagner, T., Schouten, S., Sinninghe Damsté, J.S., 2008. Climate-ocean coupling off north-West Africa during the lower albian: the oceanic anoxic event 1b. Palaeogeogr. Palaeoclimatol. Palaeoecol. 262, 157–165. https://doi.org/10.1016/j.palaeo.2008.02.014.
Holz, M., Vilas-Boas, D.B., Troccoli, E.B., Santana, V.C., Vidigal-Souza, P.A., 2017. Chapter four - conceptual models for sequence stratigraphy of continental rift successions. In: Montenari, M.B.T.-S., T (Eds.), Advances in Sequence Stratigraphy. Academic Press, pp. 119–186. https://doi.org/10.1016/bs.sats.2017.07.002.
Hunt, J.M., 1995. Petroleum Geochemistry and Geology. ISBN 0 7167 2441 3. 133(4), Second Edition, second ed., p. 743. https://doi.org/10.1017/S0016756800007755743
Hunt, J.M., Philp, R.P., Kvenvolden, K.A., 2002. Early developments in petroleum geochemistry. Org. Geochem. 33, 1025–1052. https://doi.org/10.1016/S0146-6380(02)00056-6.
Jacquin, T., Graciansky, P.-C., 2012. Transgressive/regressive (Second Order) Facies Cycles: the Effects of Tectono-Eustasy. Mesozoic and Cenozoic Sequence Stratigraphy of European Basins. SEPM Special Publication No. 60.
Jarvie, D.M., 1991. Total organic carbon (TOC) analysis. Chapter 11: geochemical methods and exploration. In: Book Title: Source and Migration Processes and Evaluation Techniques, pp. 113–118. https://doi.org/10.1306/TrHbk543C11.
Jarvie, D., 2012. Shale resource systems for oil resource systems. Shale Reserv 89–119. https://doi.org/10.1306/13321447M973489.
Jenkyns, H.C., 1980. Cretaceous anoxic events: from continents to oceans. J. Geol. Soc. London. 137, 171–188. https://doi.org/10.1144/gsjgs.137.2.0171.
Jenkyns, H.C., 2010. Geochemistry of oceanic anoxic events. Geochem. Geophys. Geosyst. 11, 1–30. https://doi.org/10.1029/2009GC002788.
Jenkyns, H.C., Wilson, P.A., 1999. Stratigraphy, paleoceanography, and evolution of cretaceous pacific guyots: relics from a greenhouse earth. Am. J. Sci. 299, 341–392. https://doi.org/10.2475/ajs.299.5.341.
Kaixuan, An, Chen, H., Lin, X., Wang, F., Yang, S., Wen, Z., Wang, Z., Zhang, G., Tong, X., 2017. Major transgression during Late Cretaceous constrained by basin sediments in northern Africa: implication for global rise in sea level. Front. Earth Sci. 11, 740–750. https://doi.org/10.1007/s11707-017-0661-0.
Kaki, C., d'Almeida, G.A.F., Yalo, N., Amelina, S., 2013. Geology and petroleum systems of the offshore Benin Basin (Benin). Oil Gas Sci. Technol.–Rev. d'IFP Energies Nouvelles 68 (2), 363–381.
Katz, B.J., 1983. Limitations of 'Rock-Eval' pyrolysis for typing organic matter. Org. Geochem. 4, 195–199. https://doi.org/10.1016/0146-6380(83)90041-4.
Katz, B.J., 2005. Controlling Factors on Source Rock Development—A Review of Productivity, Preservation, and Sedimentation Rate.
Khalifa, Z., Affouri, H., Rigane, A., Jacob, J., 2018. The Albian oceanic anoxic events record in central and northern Tunisia: geochemical data and paleotectonic controls. Mar. Petrol. Geol. 93, 145–165.
Kidder, D.L., Worsley, T.R., 2010. Phanerozoic large igneous provinces (LIPs), HEATT (haline euxinic acidic thermal transgression) episodes, and mass extinctions. Palaeogeogr. Palaeoclimatol. Palaeoecol. 295 (1–2), 162–191. https://doi.org/10.1016/j.palaeo.2010.05.036.
Klemme, H.D., Ulmishek, G.F., 1991. Effective petroleum source rocks of the world: stratigraphic distribution and controlling depositional factors. AAPG Bull. 75 (12), 1809–1851.
Lana, C.C., Arai, M., Roesner, E.H., 2002. Dinoflagelados f'osseis da seçao cret'acea marinha das bacias marginais brasileiras: um estudo comparativo entre as margens equatorial e sudeste. Simp'osio sobreo Cret'aceo do Brasil 6, 247–252.
Leopoldino Oliveira, K.M., Bedle, H., Castelo Branco, R.M.G., de Souza, A.C.B., Nepomuceno Filho, F., Normando, M.N., de Almeida, N.M., da Silva Barbosa, T.H., 2020. Seismic stratigraphic patterns and characterization of deepwater reservoirs of the Mundaú sub-basin, Brazilian Equatorial Margin. Mar. Petrol. Geol. 116, 104310. https://doi.org/10.1016/j.marpetgeo.2020.104310.
Loutit, T.S., Hardenbol, J., Vail, P.R., Baum, G.R., 1988. Condensed sections: the key to age determination and correlation of continental margin sequences. Sea-level Chang. Integr. Appr. 183–213. https://doi.org/10.2110/pec.88.01.0183.
Lü, M., Chen, K., Xue, L., Yi, L., Zhu, H., 2010. High-resolution transgressive-regressive sequence stratigraphy of Chang 8 Member of Yanchang Formation in southwestern Ordos basin, northern China. J. Earth Sci. 21, 423–438. https://doi.org/10.1007/s12583-010-0105-1.
Lüning, S., Kolonic, S., Belhadj, E.M., Belhadj, Z., Cota, L., Barić, G., Wagner, T., 2004. Integrated depositional model for the Cenomanian-Turonian organic-rich strata in North Africa. Earth Sci. Rev. 64, 51–117. https://doi.org/10.1016/S0012-8252(03)00039-4.
Mac Gregor, D.S., Robinson, J., Spear, G., 2003. Play fairways of the Gulf of Guinea transform margin. In: Arthur, T.J., MacGregor, D.S., Cameron, N.R. (Eds.), Petroleum Geology of Africa: New Themes and Developing Technologies, vol. 207. Geological Society Special Publication, London, pp. 131–150.
Macgregor, D., 2010. Understanding African and Brazilian Margin Climate, Topography and Drainage Systems, Implications for Predicting Deepwater Reservoirs and Source Rock Burial History. AAPG Search and Discovery, #10270. http://www.searchanddiscovery.com/documents/2010/10270macgregor/ndx_macgregor.pdf.
Madhavaraju, J., Lee, Y.I., Scott, R.W., González-León, C.M., Jenkyns, H.C., Saucedo-Samaniego, J.C., Ramasamy, S., 2018. High-resolution carbonate isotopic study of the Mural Formation (Cerro Pimas section), Sonora, México: implications for early Albian oceanic anoxic events. J. S. Am. Earth Sci. 82, 329–345.
Maestrelli, D., Maselli, V., Kneller, B., Chiarella, D., Scarselli, N., Vannucchi, P., Jovane, L., Iacopini, D., 2020. Characterisation of submarine depression trails driven by upslope migrating cyclic steps: insights from the Ceará Basin (Brazil). Mar. Petrol. Geol. 115, 104291. https://doi.org/10.1016/j.marpetgeo.2020.104291.
Maia de Almeida, N., Alves, T.M., Nepomuceno Filho, F., Freire, G.S.S., Souza, A.C.B., Leopoldino Oliveira, K.M., Normando, M.N., Barbosa, T.H.S., 2020. A three-dimensional (3D) structural model for an oil-producing basin of the Brazilian equatorial margin. Mar. Petrol. Geol. 122 https://doi.org/10.1016/j.marpetgeo.2020.104599.
Maia de Almeida, N., Alves, T.M., Nepomuceno Filho, F., Freire, G.S.S., Souza, A.C.B. de, Normando, M.N., Oliveira, K.M.L., Barbosa, T.H. da S., 2020a. Tectono-sedimentary evolution and petroleum systems of the Mundaú sub-basin: a new deep-water exploration frontier in equatorial Brazil. Am. Assoc. Petrol. Geol. Bull. 104, 795–824. https://doi.org/10.1306/07151917381.
Mancini, E.A., Puckett, T.M., 1998. Jurassic and cretaceous transgressive-regressive (T-R) cycles , northern Gulf of Mexico , USA. Russell J. Bertrand Russell Arch. 31–48.

Martins, L.R., Coutinho, P.N., 1981. The Brazilian continental margin. Earth Sci. Rev. 17, 87–107. https://doi.org/10.1016/0012-8252(81)90007-6.
Mascle, J., Blarez, E., 1987. Evidence for transform margin evolution from the Ivory Coast-Ghana continental margin. Nature 326, 378–381. https://doi.org/10.1038/326378a0.
Mascle, J., Blarez, E., Marinho, M., 1988. The shallow structures of the Guinea and Ivory Coast-Ghana transform margins: their bearing on the Equatorial Atlantic Mesozoic evolution. Tectonophysics 155, 193–209. https://doi.org/10.1016/0040-1951(88)90266-1.
Mascle, J., Lohmann, P., Lohmann, G.P., Clift, P., Akamaluk, T., Allerton, S., Ask, M., Barrera, E.C., Barton, E., Basile, C., Bellier, J.P., Benkhelil, J., Brantuoh, E., Edwards, R., Ewert, E., Goncalves, C., Janik, A., Holmes, M.A., Hisada, K.I., Lohmann, K.C., Morita, S., Mortera-Gutierrez, C.A., Norris, R.D., Oboh, F.E., Pletsch, T., Pickett, E.A., Ravizza, G., Shafik, S., Shin, I.C., Strand, K.O., Wagner, T., Watkins, D., 1997. Development of a passive transform margin: Côte d'Ivoire-Ghana transform margin - ODP Leg 159 preliminary results. Geo Mar. Lett. 17, 4–11. https://doi.org/10.1007/PL00007205.
Matos, R.M.D., 2000. Tectonic evolution of the equatorial south atlantic. Geophys. Monogr. 115, 331–354. https://doi.org/10.1029/GM115p0331.
Mello, M.R., Soldan, A.L., Cerqueira, R.N., Beltrami, C.V., 1984. Avaliação geoquímica da Bacia do Cear'a. Petrobr'as/Cenpes (Relat'orio interno), Rio de Janeiro, p. 1663.
Mello, M.R., Telnaes, N., Gaglianone, P.C., Chicarelli, M.I., Brassell, S.C., Maxwell, J.R., 1988. Organic geochemical characterisation of depositional palaeoenvironments of source rocks and oils in Brazilian marginal basins. Org. Geochem. 13, 31–45. https://doi.org/10.1016/0146-6380(88)90023- X.
Miceli-Romero, A., Philp, R.P., 2012. Organic geochemistry of the Woodford Shale, southeastern Oklahoma: how variable can shales. Am. Assoc. Petrol. Geol. Bull. 96, 493–517. https://doi.org/10.1306/08101110194.
Milton, N.J., Emery, D., 2009. Outcrop and well data. In: Sequence Stratigraphy, pp. 61–79. https://doi.org/10.1002/9781444313710.ch4.
Mitchum, R.M., Posamentier, H.W., 1988. Key definitions of sequence stratigraphy. AAPG Stud. Geol. 27, 11–14.
Mitchum Jr., R.M., Vail, P.R., Thompson III, S., 1977. The depositional sequence as a basic unit for stratigraphic analysis. AAPG Mem. 26 Seism. Stratigr. to Hydrocarb. Explor. 53–63.
Mohriak, W.U., Rosendahl, B.R., 2003. Transform zones in the South Atlantic rifted continental margins. Geol. Soc. Lond. Spec. Publ. 210, 211–228. https://doi.org/10.1144/GSL.SP.2003.210.01.13.
Morais Neto, J.M., Pessoa Neto, O.C., Lana, C.C., Zalán, P.V., 2003. Bacias sedimentares brasileiras: bacia do Ceará. Phoenix 5, 1–8.
Moulin, M., Aslanian, D., Unternehr, P., 2010. A new starting point for the south and equatorial Atlantic Ocean. Earth Sci. Rev. 98, 1–37. https://doi.org/10.1016/j.earscirev.2009.08.001.
Nemčok, M., Henk, A., Allen, R., Sikora, P.J., Stuart, C., 2013. Continental break-up along strike-slip fault zones; observations from the equatorial Atlantic. Geol. Soc. Spec. Publ. 369, 537–556. https://doi.org/10.1144/SP369.8.
Nijenhuis, I.A., Bosch, H.J., Damsté, J.S., Brumsack, H.J., De Lange, G.J., 1999. Organic matter and trace element rich sapropels and black shales: a geochemical comparison. Earth Planet Sci. Lett. 169 (3–4), 277–290.
Omodeo-Salé, S., Suárez-Ruiz, I., Arribas, J., Mas, R., Martínez, L., Josefa Herrero, M., 2016. Characterization of the source rocks of a paleo-petroleum system (Cameros Basin) based on organic matter petrology and geochemical analyses. Mar. Petrol. Geol. 71, 271–287. https://doi.org/10.1016/j.marpetgeo.2016.01.002.
Partington, M.A, Mitchener, B.C., Milton, N.J., Fraser, A.J., et al., 1993. Genetic sequence stratigraphy for the North Sea Late Jurassic and Early Cretaceous: distribution and prediction of Kimmeridgian–Late Ryazanian reservoirs in the North Sea and adjacent areas. Geological Society, London, Petroleum Geology Conference series 4, 347–370. https://doi.org/10.1144/0040347.
Pasley, M.A., 1991. Organic Matter Variation within Depositional Sequences; Stratigraphic Significance and Implication to Petroleum Source Rock Prediction.
Pasley, M.A., Hazel, J.E., 1990. Use of Organic Petrology in Sequence Stratigraphic Interpretations: Example from the Eocene-Oligocene Boundary Section, St. Stephens Quarry, Washington County, Alabama. AAPG Bulletin (American Association of Petroleum Geologists), USA), p. 74. CONF-9010204–).
Pasley, M.A., Gregory, W.A., Hart, G.F., 1991. Organic matter variations in transgressive and regressive shales. Org. Geochem. 17, 483–509.
Paytan, A., Kastner, M., Campbell, D., Thiemens, M.H., 2004. Seawater sulfur isotope fluctuations in the Cretaceous. Science 304 (5677), 1663–1665.
Pedersen, T.F., Calvert, S.E., 1990. Anoxia vs. productivity: what controls the formation of organic-carbon-rich sediments and sedimentary rocks? AAPG Bull. 74 (4), 454–466.
Pellegrini, B. da S., Ribeiro, H.J.P.S., 2018. Exploratory plays of Par'a-Maranhao and Barreirinhas basins in deep and ultra-deep waters, Brazilian Equatorial Margin. Brazilian J. Geol. 48, 485–502. https://doi.org/10.1590/2317-4889201820180146, 1154.
Peng, J., Pang, X., Peng, H., Ma, X., Shi, H., Zhao, Z., Xiao, S., Zhu, J., 2016. Geochemistry, origin, and accumulation of petroleum in the Eocene Wenchang formation reservoirs in Pearl river mouth basin, south China sea: a case study of HZ25-7 oil field. Mar. Petrol. Geol. https://doi.org/10.1016/j.marpetgeo.2016.08.007.
Pessoa Neto, O.C., 2004. Blocos basculados truncados por discordancia angular: liçoes aprendidas em trapeamento combinado de hidrocarbonetos, Bacia do Cear'a, Nordeste do Brasil. Boletim de Geocien. Petrobras v 12, 59–71.
Pessoa Neto, O. da C., Soares, U.M., Silva, J.G.F. da, Roesner, E.H., Florencio, C.P., Souza, C.A.V. de, 2007. Bacia potiguar. Bol. Geociencias Petrobras 15, 357–369.
Peters, K.E., 1986. Guidelines for evaluating petroleum source rock using programmed pyrolysis. Am. Assoc. Petrol. Geol. Bull. 70, 318–329. https://doi.org/10.1306/94885688-1704-11D7-8645000102C1865D.
Regali, M.S.P., 1989. A idade dos evaporitos da plataforma continental do Ceará. Brasil. Boletim do IG-USP, Publ. Espec. 7, 139–143.
Rios, I.A.L., Picanço, F.J., 2018. Anuário do Instituto de Geociências - UFRJ Arcabouço Estratigráfico da Seção Drifte em Águas Profundas da Sub-Bacia de Mundaú, Bacia do Ceará, e sua Relação com a Datação de Eventos Vulcânicos stratigraphic framework of the Mundaú Sub-Basin ' s Drift Se, 41, 152–166.
Rodrigues, R., 1983. Utilização de marcadores biológicos na correlação dos óleos da Bacia do Ceará e parte emersa da Bacia Potiguar. Bol. Tec. Petrobras 950, 163–179.
Rodrigues, R., Pereira, E., Bergamaschi, S., Bastos, L.P.H., 2019. Chapter Four - stable isotopes as a tool for stratigraphic studies: insights from the Brazilian sedimentary record. In: Montenari, M.B.T.-S., T (Eds.), Case Studies in Isotope Stratigraphy. Academic Press, pp. 133–164.
Sabatino, N., Coccioni, R., Manta, D.S., Baudin, F., Vallefuoco, M., Traina, A., Sprovieri, M., 2015. High-resolution chemostratigraphy of the late Aptian–early Albian oceanic anoxic event (OAE 1b) from the Poggio le Guaine section (Umbria–Marche Basin, central Italy). Palaeogeogr. Palaeoclimatol. Palaeoecol. 426, 319–333.
Santos Neto, E.V.D., Hayes, J.M., 1999. Use of hydrogen and carbon stable isotopes characterizing oils from the Potiguar Basin (onshore), Northeastern Brazil. AAPG Bull. 83 (3), 496–518.
Schiefelbein, C.F., Zumberge, J.E., Cameron, N.C., Brown, S.W., 2000. AAPG Memoir 73, Chapter 2: Geochemical Comparison of Crude Oil along the South Atlantic Margins.
Schlanger, S.O., Jenkyns, H.C., 1976. Cretaceous oceanic anoxic events: causes and consequences. Geol. Mijnbouw 55, 179–184.
Schlanger, S.O., Jenkyns, H.C., 2007. Cretaceous oceanic anoxic events: causes and consequences. Netherlands J. Geosci./Geol. Mijnbouw (Classic Papers).
Schlanger, S.O., Arthur, M.A., Jenkyns, H.C., Scholle, P.A., 1987. The Cenomanian-Turonian Oceanic Anoxic Event, I. Stratigraphy and distribution of organic carbon-rich beds and the marine δ13C excursion. Geol. Soc. Lond. Spec. Publ. 26 (1), 371–399. https://doi.org/10.1144/GSL.SP.1987.026.01.24.
Schön, J.H., 2015. Physical Properties of Rocks: Fundamentals and Principles of Petrophysics. Elsevier.
Shekarifard, A., Daryabandeh, M., Rashidi, M., Hajian, M., 2019. International journal of coal geology petroleum geochemical properties of the oil shales from the early cretaceous garau formation, Qalikuh locality, Zagros mountains, Iran. Int. J. Coal Geol. 206, 1–18. https://doi.org/10.1016/j.coal.2019.03.005.
Slatt, R., 2013. Sequence Stratigraphy of the Woodford Shale and Application to Drilling and Production. https://doi.org/10.1016/j.jngse.2012.01.008. Search Discov. #50792 50792.
Slatt, R.M., O'Brien, N.R., 2011. Pore types in the Barnett and Woodford gas shales: contribution to understanding gas storage and migration pathways in fine-grained rocks. Am. Assoc. Petrol. Geol. Bull. 95, 2017–2030. https://doi.org/10.1306/03301110145.
Slatt, R.M., Rodriguez, N.D., 2012. Comparative sequence stratigraphy and organic geochemistry of gas shales: commonality or coincidence ? J. Nat. Gas Sci. Eng. 8, 68–84. https://doi.org/10.1016/j.jngse.2012.01.008.
Soares, E.F., Zalán, P.V., Figueiredo, J.J.P., Trosdtorf Jr., I., 2007. Bacia do par'a-maranhao. Bol. Geociencias Petrobras 15 (2), 321–330.
Soares, D.M., Alves, T.M., Terrinha, P., 2012. The breakup sequence and associated lithospheric breakup surface: their significance in the context of rifted continental margins (West Iberia and Newfoundland margins, North Atlantic). Earth Planet Sci. Lett. 355, 311–326.
Soua, M., 2014. Paleozoic oil/gas shale reservoirs in southern Tunisia: an overview. J. Afr. Earth Sci. 100, 450–492. https://doi.org/10.1016/j.jafrearsci.2014.07.009.
Soua, M., 2016. Cretaceous oceanic anoxic events (OAEs) recorded in the northern margin of Africa as possible oil and gas shale potential in Tunisia: an overview. Int. Geol. Rev. 58, 277–320. https://doi.org/10.1080/00206814.2015.1065516.
Soua, M., Tribovillard, N., 2007. Modèle de sédimentation au passage Cénomanien/Turonien pour la formation Bahloul en Tunisie. Compt. Rendus Geosci. 339, 692–701. https://doi.org/10.1016/j.crte.2007.08.002.
Souza, A.C.B., Nascimento Jr., D.R., Batezelli, A., Nepomuceno Filho, F., Leopoldino Oliveira, K.M., Maia de Almeida, N., Normando, M.N., Barbosa, T.H.S., 2021. Geochemical constraints on the origin and distribution of Cretaceous source rocks in the Ceará basin, Brazilian Equatorial margin. J. S. Am. Earth Sci. 107 https://doi.org/10.1016/j.jsames.2020.103092.
Swanson, V.E., 1960. Oil Yield and Uranium Content of Black Shales. https://doi.org/10.3133/pp356A. Professional Paper.
Szatmari, P., Françolin, J.B.L., Zanotto·O, Wolf, S., 1987. Evolução Tectônica da Margem Equatorial Brasileira. Rev. Bras. Geociencias 17, 180–188.
Tamara, J., McClay, K., Hodgson, N., 2020. Crustal structure of the central sector of the NE Brazilian equatorial margin. In: McClay, K.R., Hammerstein, J.A. (Eds.), Passive Margins: Tectonics, Sedimentation and Magmatism, vol. 476. Geological Society, London, Special Publications. https://doi.org/10.1144/SP476-2019-54.
Tayson, R.V., 2001. Sedimentation rate, dilution, preservation and total organic carbon: some results of a modelling study. Org. Geochem. 32, 333–339. https://doi.org/10.1016/S0146-6380(00)00161-3.
Tiraboschi, D., Erba, E., Jenkyns, H.C., 2009. Origin of rhythmic Albian black shales (Piobbico core, central Italy): calcareous nannofossil quantitative and statistical analyses and paleoceanographic reconstructions. Paleoceanography 24, 1–21. https://doi.org/10.1029/2008PA001670.
Tissot, B.P., Welte, D.H., 1984. From kerogen to petroleum. Pet. Form. Occur. 160–198 https://doi.org/10.1007/978-3-642-87813-8_10.

Tissot, B., Demaison, G., Masson, P., Delteil, J.R., Combaz, A., 1980. Paleoenvironment and petroleum potential of middle Cretaceous black shales in Atlantic basins. Am. Assoc. Petrol. Geol. Bull. 64, 2051–2063. https://doi.org/10.1306/2f919738-16ce-11d7-8645000102c1865d.

Trindade, L.A.F., Brassell, S.C., Neto, E.S., 1992. Petroleum migration and mixing in the Potiguar basin, Brazil. AAPG Bull. 76 (12), 1903–1924.

Trosdtorf Jr., I., Zalán, P.V., Figueiredo, J.J.P., 2007. Bacia de Barreirinhas. Bol. Geociencias Petrobras 15, 331–339.

Turgeon, S.C., Creaser, R.A., 2008. Cretaceous oceanic anoxic event 2 triggered by a massive magmatic episode. Nature 454 (7202), 323–326.

Tuttle, M.L., Charpentier, R.R., Brownfield, M.E., 1999. The Niger Delta Petroleum System: Niger Delta Province, Nigeria, Cameroon, and Equatorial Guinea. US Department of the Interior, US Geological Survey, Africa.

Vail, P.R., Mitchum Jr., R.M., Thompson III, S., 1977. Seismic Stratigraphy and Global Changes of Sea Level: Part 4. Global Cycles of Relative Changes of Sea level.: Section 2. Application of seismic reflection configuration to stratigraphic interpretation.

Van Wagoner, J.C.R.M., Mitchum, J., 2003. Seismic Stratigraphy Interpretation Using Sequence Stratigraphy: Part 2: Key Definitions of Sequence Stratigraphy. https://doi.org/10.1306/bf9ab166-0eb6-11d7-8643000102c1865d.

Van Wagoner, J.C., Mitchum, R.M., Posamentier, H.W., 1988. Key definitions of sequence stratigraphy. AAPG Stud. Geol. 27, 11–14.

Veeken, P.C., 2006. Seismic Stratigraphy, Basin Analysis and Reservoir Characterisation. Elsevier, ISBN 9780080466309, p. 522.

Wagner, T., Wallmann, K., Herrle, J.O., Hofmann, P., Stuesser, I., 2007. Consequences of moderate ~ 25,000 yr lasting emission of light CO2 into the mid-Cretaceous ocean. Earth Planet Sci. Lett. 259, 200–211. https://doi.org/10.1016/j.epsl.2007.04.045.

Wignall, P.B., 1991. Model for transgressive black shales? Geology 19, 167–170. https://doi.org/10.1130/0091-7613(1991)019<0167:MFTBS>2.3.CO;2.

Zalán, P.V., Nelson, E.P., Warme, J.E., Davis, T.L., 1985. The Piaui Basin Rifting and Wrenching in an Equatorial Atlantic Transform Basin.

Zobaa, M.K., Oboh-Ikuenobe, F.E., Ibrahim, M.I., 2011. The Cenomanian/Turonian oceanic anoxic event in the Razzak Field, north Western Desert, Egypt: source rock potential and paleoenvironmental association. Mar. Petrol. Geol. 28, 1475–1482. https://doi.org/10.1016/j.marpetgeo.2011.05.005.